國立臺灣大學工學院化學工程學系

碩士論文

Department of Chemical Engineering

College of Engineering

National Taiwan University

Master Thesis

可撓式電致變色元件之噴墨混色與圖樣化研究

Printed Multi-Color High-Contrast Flexible

Electrochromic Devices

陳柏翰

Bo-Han Chen

指導教授：廖英志博士

Advisor: Ying-Chih Liao, Ph.D.

中華民國 104 年 6 月

June, 2015

國立臺灣大學碩(博)士學位論文
口試委員會審定書
可撓式電致變色元件之噴墨混色及圖樣化研究
Printed Multi-Color High-Contrast Flexible Electrochromic Devices

本論文係陳柏翰君（R02524059）在國立臺灣大學化工學系 所完成之碩（博）士學位論文，於民國 104 年 6 月 26 日承下列考試委員審查通過及口試及格，特此證明

口試委員：

廖英志 （簽名）

（指導教授）

石國川

林正嵐

樋口昌芽

閻子輝

系主任、所長 王大銘 （簽名）

（是否須簽章依各院系所規定）

#

Acknowledgements

中文摘要

本論文利用一種簡單且迅速的噴墨直寫技術來製作多色彩可撓曲式圖樣化電致變色元件。此元件係利用一種電致變色超分子聚合物 (Metallo-supramolecular polymers, MEPE) 製成，相較於傳統電致變色材料，MEPE 具有高對比度、高穩定性及高著色效率等特性。由於此聚合物為水溶性，因此可將其製作成墨水，並利用噴墨技術直接噴塗於導電基材上。

首先，為了製作出平整且緻密的變色材料薄膜，使用不同的液滴排列並探討其對薄膜樣態的影響。找出均勻噴塗的方式後，在透明導電基材 ITO-PEN 上製作薄膜並以循環伏安法及光譜儀測量其電化學與光學性質。與先前之文獻做比較，電致變色材料薄膜之吸收峰值與氧化還原電位並無因不同製程而改變。印製而成的變色薄膜接著與固態電解質搭配，組合成可撓曲式電致變色元件。此電解質是由高沸點之非揮發性離子液體 (EMIBTI) 與高分子 (PVDF-HFP) 製作而成。當改變施加的電壓時 (-3.0~3.0 V)，此元件可在兩秒鐘內著色並具有相當高的對比度以及著色效率。在 580 nm 之波長下，其穿透度變化為 40.1% 並且具有 445 cm^2C^{-1} 之高著色效率。當此元件彎曲時，其穿透度變化仍可達 30.1% 且著色時間不變，是相當好的展現。

接著，利用噴墨技術將兩種不同顏色之 MEPE 混合成一系列不同顏色以及圖樣化之電致變色薄膜。同樣地，利用光譜儀及循環伏安法探討混合後之特性。可發現兩者之吸收光譜會線性疊加，進而顯現不同的顏色。與先前文獻使用合成調整顏色不同的是：藉由噴墨技術混合的變色薄膜，其氧化還原電位並不會因兩種金屬離子的交互作用而偏移。最後，本論文利用噴墨技術可在不需遮罩的情形下精確噴印出所設計的圖樣之特點，搭配兩種變色材料製作圖樣化之電致變色元件，為此製程在軟性顯示器的應用提供進一步的可能性。

關鍵字：電致變色、印刷電子、噴墨技術、金屬配位超分子、顯示器

ABSTRACT

In this thesis, multi-colored electrochromic (EC) thin film devices were prepared by a direct-writing method. Metallo-supramolecular polymers (MEPE) solutions with two primary colors were inkjet-printed digitally on flexible electrodes. Uniform EC thin films are fabricated via inkjet printing. Further, by digitally controlling print dosages of each species, colors of the printed EC thin film patterns can be adjusted directly without pre-mixing or synthesizing new materials. The printed EC thin films were then laminated with a solid transparent thin film electrolyte and a transparent conductive thin film to form an electrochromic device (ECD). After applying a DC voltage, the printed ECDs exhibited a great contrast with a transmittance change (ΔT) of 40.1% and a high coloration efficiency of 445 cm^2C^{-1} at 580 nm within a short darkening time of 2 s. The flexible ECDs can also be made base on ITO-PEN and showed same darkening time of 2 s and still have a high ΔT of 30.1% under bending condition. In summary, this study demonstrated the feasibility to fabricate display devices with different color set up by all-solution process, and can be further extended to other types of displays.

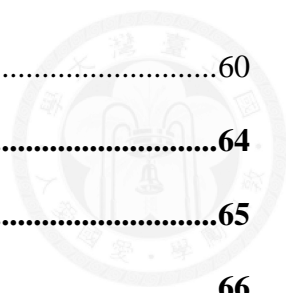Key words: Metallo-Supramolecular, Display, Electrochromic, Printing Electronics, Inkjet Printing

Table of Contents

List of Figures

List of Tables

Chapter 1 Introduction

1.1 Preface

Flexible electronics have been developed for decades since the early stage of the flexible solar cells array made up with silicon based thin film transistor[1] to the polymer based organic light emitting diode.[2] In recent years, the rapid development of flexible electronics led to the continued progress of large-area electronics which have widely used in flat panel displays, medical imaging sensors and e-books.[3, 4] Flexible electronics have some fascinated properties including lightweight and robust which make it much portable comparing to those rigid silican based electronics.[5]

Recently, printed electronics began to be extensively studied since it has the ability of producing large-scale flexible electronics components with low cost. However, printed electronics is still at a preliminary stage, a number of technical difficulties were faced including electrical conductivity, adhesion and flexibility.[6, 7] There are still a lot of room for improvement, therefore, the development of new manufacturing processes to improve component reliability plays an important roles for the development of flexible electronics technology.

Flexible display is also one of the popular themes which researchers pay a lot of attention to. This kind of device has been produced with different techniques such as

organic light emitting diode (OLED), electrophoretic, electrowetting and electrochromic

(EC).[8-10] The competition of ECDs in display is a big issue due to other techniques,

However, ECDs still hold advantages such as multi-color feasibility, low energy

consumption and low driving voltage comparing to other non-emissive displays.[11]
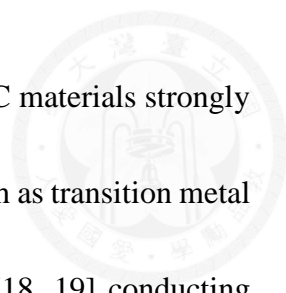
Table 1.1 Comparison of ECDs with other mon-emissive displays.[11]

Property	Electro chromic displays (ECDs)	Electro phoretic (EP) displays	Field effect liquid crystal (FELC) displays	Dynamic scattering liquid crystal (DSLC) displays	Dipole suspension (DS) displays
Viewing angle	Wide	Wide	Narrow	Narrow	Narrow
Optical mode	T^a, R^b, P^c	R	T, R, P	T, R, P	T, R
Color	Two or more	Two	B/W or dye	B/W	B/W
Resolution	Electrode limited	Electrode limited	Electrode limited	Electrode limited	Electrode limited
Operating mode	dc pulse	dc pulse	ac	ac	ac
Voltage (V)	0.25–20	30–80	2–10	10–30	2–30
Power ($\mu W/cm^2$)	1–10	15	<0.1	1–10	1–10
Energy (mJ/cm^2)	10–100	6×10^{-4}			
Memory	Yes	Yes	No/yes	No/yes	No
Threshold	Poor	No	Poor	Poor	Poor
Contrast					
Write time (ms)	100–1000	60	20	20	20
Erase time (ms)	100–500	30	1–500	100	30
Operating life	10^5–10^6 cycles		$>2 \times 10^4$ h	$>1 \times 10^4$ h	

[a] Transmission. [b] Reflection. [c] Projection.
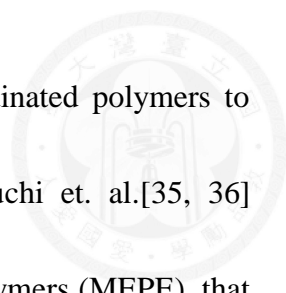
1.2   Objective

Electrochromic devices (ECDs) are systems with electrically controllable light-

transmissive or light-reflective properties, and have been widely proposed in many

commercial applications, such as anti-glare rear-view mirrors, sunglasses, protective

eyewear, and 'smart windows' for aircrafts or buildings.[12] In the fabrication of ECD,

electrochromic (EC) materials, which can switch colors electrochemically, are usually

coated as thin films on transparent electrodes for fast color changes or rapid optical

2
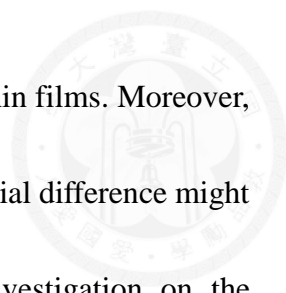
responses to electrical stimulus.[11] The color change behavior of EC materials strongly

depends on their intrinsic properties and thus many EC materials, such as transition metal

oxides,[13-15] Prussian blue and its analogues,[16, 17] viologens,[18, 19] conducting

polymers,[20-22] metallopolymers[23, 24] and metal phthalocyanines,[25-27] have been

synthesized to meet various color or optical requirements. Typically, EC thin films can be

prepared by various coating processes, [11-30] including chemical vapor deposition, sol-

gel, RF-sputtering, spin coating and spray coating. However, these coating methods

usually require masks to create thin film patterns and hence potentially result in enormous

material wastes during the fabrication of commercial devices. To reduce material

consumption with a faster process for the fabrication of ECDs, digital inkjet technology

has been developed to print EC patterns on transparent conductive thin film.[31, 32]

These printed ECDs have square pixel sizes as small as 500 µm × 500 µm, and are able

to exhibit interactive color switching for image display applications.[31]

Besides thin film deposition, another technical challenge for ECD fabrication lies in

its color adjustment. Regularly, an EC material can only absorb a specific wavelength and

give a specific color with various tones depending on the voltage applied. Thus, these EC

thin films can only yield monotonic color change. To produce a variety of color

possibilities for EC materials, chemists have tried various chemical synthetic methods,

such as side chain functionalization[33] and copolymerization.[34] Besides polymer

synthesis, one can also utilize the ligand/ion interactions in coordinated polymers to synthesis EC materials with different adsoptions. Recently, Higuchi et. al.[35, 36] synthesized a new class of EC material, metallo-supramolecular polymers (MEPE), that exhibit electrochromic behavior based on the redox reaction of the inserted metal ions. Due to the metal-to-ligand change transfer (MLCT) effect of MEPE,[37] the polymer materials show various colors depending on the conjugated metal ions. Consequently, by simply replacing the inserted metal ion, one can easily obtain EC materials of similar molecular structures having different colors.[38] Furthermore, by mixing Fe(II) and Ru(II) ions at various ratios in the MEPE synthesis, Hu et al. obtained EC materials showing multi-electrochromism.[39] These MEPEs exhibit a high transmittance change up to 60% at 580 nm with a fast response time of a few seconds.[39] Although EC materials can be synthesized to offer a variety of colors, the chemical synthesis still takes time. Thus, it is of practical interests to investigate color variation by mixing EC materials. Generally, the absorbance of a binary EC mixture can be resulted from the superposition of the individual absorbance. As shown recently by Bulloch et al., mixing CMY representative EC polymers in solution at various ratios can yield in thin films with predictable colors.[40] However, the pre-mixing ink and spray coating would lead to material waste and inconvenience in color adjustment. To allow the color adjustment becomes more flexible with much less material consumption, inkjet printing skills with digital color

adjustment method is proposed in this work to create patterned EC thin films. Moreover, when two different EC materials are mixed together, the redox potential difference might involve complex electrochemical reactions. Thus, a thorough investigation on the electrochemical properties of EC mixtures is needed and will be extensively discussed in this study.

Here, a simple direct writing method is developed to investigate the feasibility of applying digital color adjustments to print EC thin film patterns. To obtain the needed inks for the solution process, compatible solvent were chosen. In the printing process, MEPE solutions with two primary colors are inkjet-printed digitally on flexible electrodes to create a series of multi-color EC thin films without pre-mixing or synthesizing new materials. The electrochromic properties, such as redox potential, UV-vis absorption, coloration efficiency and response time, will be explored to evaluate the performance of these printed thin films with binary EC materials. The electrochemical stability of the fabricated ECD under bending conditions will also be demonstrated to ensure the needed darkening-bleaching cycles for flexible display applications. Finally, an ECD with multi-color patterns is also fabricated to demonstrate the ability of precise deposition for the inkjet printing process.

1.3   Thesis structure

In the first chapter, the preface of flexible electronics and the introduction of electrochromic device were summarized. The development of the electrochromic materials and the mechanism of color switching will be talked about in chapter 2. In this chapter, inkjet printing technology will also be introduced briefly. In chapter 3, flexible ECDs fabricated with inkjet printed EC thin films will be produced and the properties of them will be examined under various conditions. Multi-color ECDs will be fabricated and the electrochemical properties of them will also be discussed in chapter 4. A short conclusion will be provided in chapter 5. To show the possibility of the further applications, an all-printed polymer based flexible EC display will be demonstrated in chapter 6.

Chapter 2 Literature Review

2.1 Electrochromic

Chemical species that can switch between different colours electrochemically are said to be elecrtrochromic (EC) and have been widely studied for more than 40 years. The colour change is commonly between a transparent (also called bleached) state and a coloured state, or between two coloured states. Electrochromism are exhibited by a number of materials, both inorganic and organic liquids and solids. Electrochromism is a reversible color change in material caused by an applied electric field or current. This change can be due to the formation of color centers (or defect complexes) of an electrochemical reaction that produces a colored compound. For example, in an inorganic solid the ion-insertion reaction might be:

Cathodic $MO_y + xA^+ + xe^- \rightleftarrows A_xMO_y$, colored when reduced,

Where $A^+ = H^+, Li^+, Na^+, Ag^+$.

Anodic $MO_y + xA^- + xh^+ \rightleftarrows A_xMO_y$, colored when oxidized,
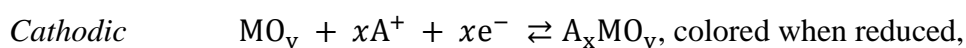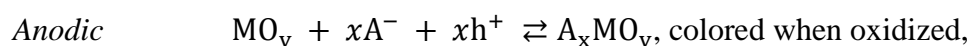
Where $A^- = F^-, CN^-, OH^-/H^+$ and x is generally $0 < x < 1$.

An electrochromic device can consist of many configurations depending on property requirements. The basic elements of an electrochromic device are: two conductor layers to inject charge, an active electrochromic layer, an electrolyte or ion conductor (which

may in some cases be an insulator) and an ion storage media which may be the integral

part of the conductive layer.
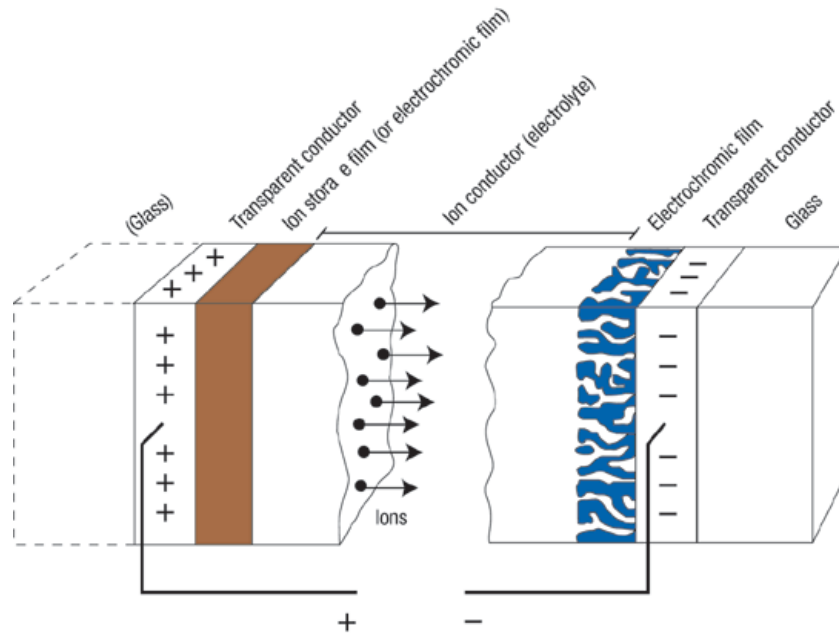
Figure 2.1 Basic elements of an electrochromic device.[41]

This sandwich configuration allows a reversible chemical reaction to cycle between the

electrochromic material and ion storage media, which simultaneous injection of electrons

or holes and protons or ions, depending on the material.

Whilst many type of chemical species exhibit electrochromism, only those with

favourable EC performance parameters are potentially useful in commercial applications.

Thus, most applications require EC materials with a high contrast ratio, colouration

efficiency (absorbance change/charge injected per unit area), cycle life, and write-erase

efficiency (% of the originally formed colouration that may be subsequently electro-

bleached). Whereas displays need fast response times, by contrast 'smart windows' can

tolerate response times of up to several minutes.

Traditionally, EC materials have been divided into three categories: (i) metal oxides,

e.g., tungsten oxide (WO_3) or nickel oxide (NiO); (ii) transition metal complexes, e.g.,

Prussian blue and its analogs; (iii) organic molecules or polymers, e.g., viologen and

poly(3,4-ethylenedioxythiophene) (PEDOT). The following are schemes of viologen and

PEDOT.
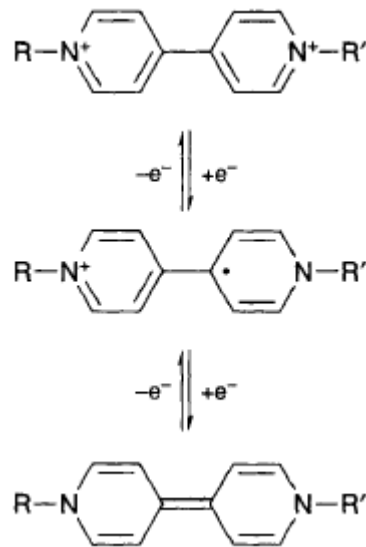
Figure 2.2 Various charge states of Viologen.[12]
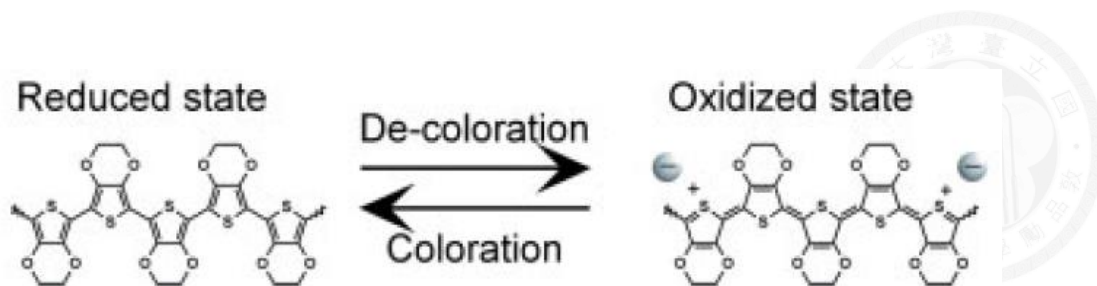
Figure 2.3 Coloration and De-coloration of PEDOT.[42]

In the past decade, a new type of EC material—metallo-supramolecular—has attracted attention and shown benefits as both inorganic and organic materials. The synthesis of various functional organic ligands with a single metal ion (Fe, Ru or Co) for application to electronic papers and smart windows has been reported. Reports also show that different metal centres can directly affect polymer characteristics, including viscosity, magnetic moment, fluorescence, and even electrochromism.

In general, organic polymers are synthesized via the polymerization of monomers, which is accompanied by the formation of covalent bonds. In contrast, metallo-supramolecular polymers,[36] which are synthesized via the 1:1 complexation of metal ions and ditopic organic ligands, are a new type of polymers, in which the polymer backbone consists of coordination bonds. The most distinguished difference in the polymer structure between the conventional organic polymers and metallo-supramolecular polymers is that the chain length of metallo-supramolecular polymers is not fixed in solution unlike that of conventional polymers because the complexation is an

equilibrium reaction.
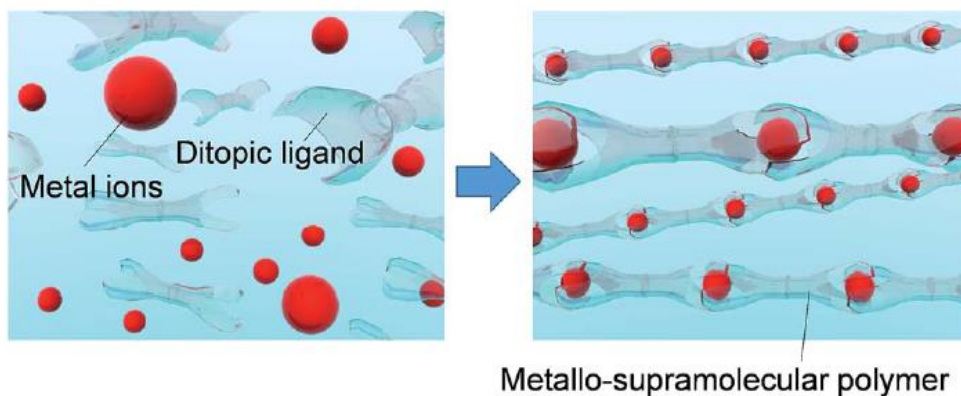
Figure 2.4 Metallo-supramolecular polymer formation.[37]

The color change of this material comes from the intramolecular MLCT (metal to ligand charge transfer). The MLCT in the visible region occurs from the HOMO (the highest occupied molecular orbital) of the metal ions to the LUMO (the lowest unoccupied molecular orbital) of the ligand in the complex moieties of the polymers. The colour of metallo-supramolecular polymers is controllable by selecting the metal ions species with different HOMO potentials or altered the ditopic organic ligands with different LOMO potentials. Various colours can be realized by the proper combinations of metal ions and ditopic ligands in the metallo-supramolecular polymer synthesis.
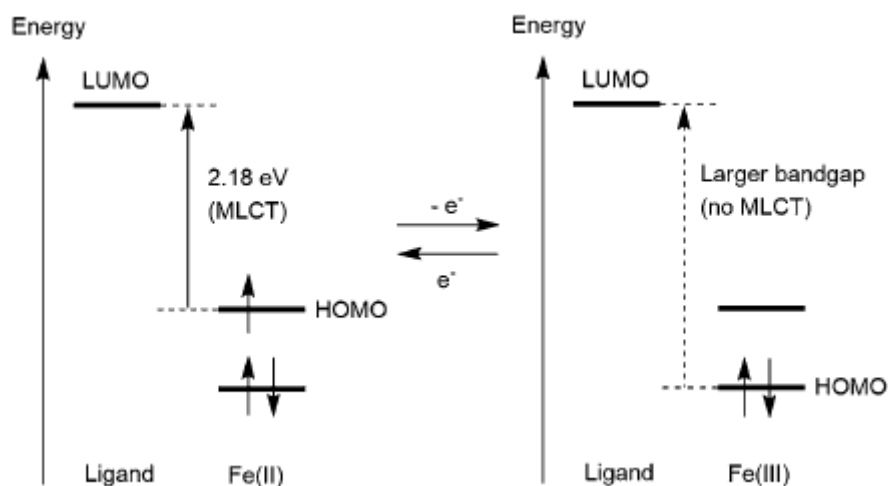
Figure 2.5 A possible mechanism for the electrochromic change in FeMEPE.

2.1.1　Transmittance Attenuation

Electrochromic contrast is probably the most important factor in evaluating an electrochromic material. It is often reported as a percent transmittance (ΔT) at a specified wavelength where electrochromic materials has the highest optical contrast. For some applications, it is more useful to report a contrast over a specific range rather than a single wavelength. To obtain an overall electrochromic contrast, measuring the relative luminance change provides more realistic contrast values since it offers a perspective on transmissivity of a material as it relates to the human eye perception of transmittance over the entire visible spectrum.

2.1.2　Coloration Efficiency

The coloration efficiency, CE (λ), (also referred to as electrochromic efficiency) is a

practical tool to measure the power requirements of an electrochromic material. In essence, it determines the amount of optical density change (ΔOD) induced as a function of the injected/ejected electronic charge (Q_d), i.e., the amount of charge necessary to produce the optical change. It is given by the following equation:
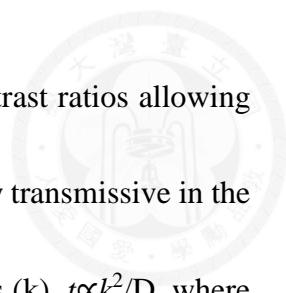
$$\eta = \frac{\Delta OD}{Q_d} = \log\frac{T_b}{T_c}\bigg/Q_d \qquad \textbf{(Eq. 2-1)}$$

Where η (cm^2/C) is the coloration efficiency at a given ΔOD and T_b and T_c are the bleached and colored transmittance values, respectively. The coloration efficiency is measured by a spectro-electrochemistry method.

2.1.3 Switching Speed

Switching speed is often reported as the time required for the coloring/bleaching process of an EC material. It is important especially for applications such as dynamic displays and switchable mirrors. The switching time of electrochromic materials is dependent on several factors such as the ionic conductivity of the electrolyte, accessibility of the ions to the electroactive sites (ion diffusion in thin films), magnitude of the applied potential, film thickness, and the morphology of the thin film. The sub-second switching rates are easily attained today using polymers and composites containing small organic

electrochromes. Many electrochromic applications require high-contrast ratios allowing devices to be prepared that are opaque in one state while being highly transmissive in the other. The switching time is proportional to the square film thickness (k), $t \propto k^2/D$, where D is the diffusion coefficient of ions dependent on the solvent, ion concentration and applied voltage.

2.2   Flexible Electronics and Printing Technology

Recently, scientists have dedicated into the conductive circuit on polymers for large scale and low cost flexible electronics.[7, 43-47] Traditional etching and vacuum metal coating technology are inevitable in the development processes. Moreover, many fabrication methods need molds to produce flexible electronics, such as screen printing[48, 49], inkjet printing[50, 51], letterpress printing[52], gravure printing[53, 54], lithography[55, 56] and micro contact printing[57, 58]. Among these printing methods, inkjet printing technology has received considerable attention recently.

Table 2.1 Comparison between different processes.
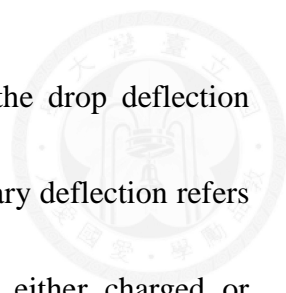
Method	Temperature	Mask	Vacuum	Scale
Chemical Vapor Deposition	High	Yes	Yes	Small
RF-Sputtering	High	Yes	Yes	Small
Spin Coating	Low	Yes	No	Small
Spray Coating	Medium	Yes	No	Large
Electrochemical Deposition	Low	Yes	No	Large
Inkjet Printing	Low	No	No	Large

The core concept of inkjet technology is a fluid dynamics of instability that is called Rayleigh instability.[59] The concept of inkjet printing originated in the 19th century, and starting in the early 1950s this technology was first extensively developed.[60] Inkjet printing technology that could reproduce digital images generated by computers was developed in the late 1970s. In accordance with the droplet control, there are two main technologies in use in contemporary inkjet printers: continuous (CIJ) mode and Drop-on-demand (DOD) mode.

2.3   Classification of Inkjet Printing Technology

2.3.1   Continuous Mode[61-64]

The continuous mode of inkjet printing system has been employed in the first

developed printer, which can be divided into two categories by the drop deflection methodology, binary-deflection and multiple-deflection system. Binary deflection refers to a continuous printing process where the ejected droplets are either charged or uncharged. The uncharged droplets will be directed into a catcher for recycling, eventually. In contrast, multiple deflection refers to that all droplets are charged but with different magnitude. The uncharged and the charged droplets are recycled into the reservoir and fly along various traces depends on the magnitude of the charge, respectively. However, it is complicated mechanism of droplet deflection and unreliable droplet recycle system make the continuous mode of inkjet printing complex and hard to control. Therefore, the drop-on-demand system has become a more popular approach because of the conceptual simplicity.

2.3.2 Drop-on-demand Mode[61-65]

Demand mode does not required recirculation or waste working fluid, as does continuous mode, because the droplets are create "on demand" with control signals. Many of the drop-on-demands of inkjet printing system were invented, developed, and produced in the 1970's and 1980's, of which piezoelectric and thermal bubble jet are the two major categories. In the piezoelectric printer, on the application of the voltage plus, ink drops are ejected by a pressure wave created by mechanical motion of piezoelectric ceramic actuators. In 1979, Canon and Hewlett-Packard (HP) invented a method where ink drops

16

were ejected from the nozzle by the growth and collapse of a water vapor bubble on the top surface of a small heater located near the nozzle. This technology is called thermal bubble jet.

The thermal bubble jet has reached an enormous success in market today due to its characteristics of cheap price and mass production by semi-conductor manufacture. However, the ink is limited because of the heater located near the nozzle. On the contrary, the available ink for the piezoelectric jet has a wide range of choices. Therefore, the piezoelectric nozzles have been mainly applied to the electrical and biological sensors. Besides the two printing methods discussed before, there are still electrostatic and acoustic ink-jet methods. But both the electrostatic inkjet and acoustic inkjet method are still in development stage and few commercial products available.

Chapter 3 Inkjet Printing EC device
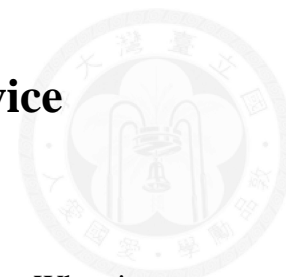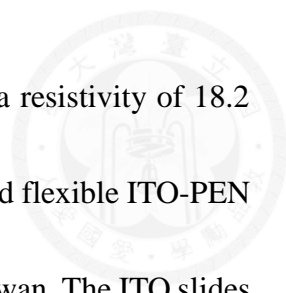
Many techniques have been used in the fabrication of EC devices. When it comes to the fabrication of flexible electronics, some of them are not suitable since the polymer substrates would be destroyed in those high temperature process. Inkjet printing process can produce EC thin film with less material consumption and does less harm to the substrate in room temperature. In this chapter, inkjet printing technology is used to produce EC thin films on the flexible conductive substrate. The performance of the ECDs fabricated with the printed EC thin films will also be examined under various condition.

3.1 Experimental

3.1.1 Materials

Acetone, methanol, acetonitrile (ACN), lithium perchlorate (LiClO$_4$), 4',4''''-(1,4-Phenylene)-bis(2,2':6',2''-terpyridine) (97%), iron(II) acetate (Fe(OAc)$_2$, >99.99%), cis-tetrakis(dimethylsulfoxide)dichlororuthenium(II) (RuCl$_2$(DMSO)$_4$, 98%), and poly(vinylidenefluoride-*co*-hexafluoropropylene) (PVDF-HFP, MW 400,000, pellets) were purchased from Sigma Aldrich, USA. 1-ethyl-3-methylimidazolium-bis(trifluoromethylsulfonyl) amide (EMIBTI, 99%) was purchased from UniRegion Bio-

Tech Co., Taiwan. Deionized water (Millipore Milli-Q grade) with a resistivity of 18.2

$M\Omega$ cm^{-1} was used in the experiments. ITO-glass (R_{sh} = 6.8 $\Omega/\square$) and flexible ITO-PEN

slides (R_{sh} = 35 $\Omega/\square$) were purchased from Yu-Yi Enterprise Co., Taiwan. The ITO slides

(3.0 × 4.0 cm^2) were cleaned by rinsing sequentially with DI water and ethanol in

ultrasonic bath (DELTA DC300H), and dried in a vacuum oven.

3.1.2　Preperation of EC Inks

MEPE inks in two different color were prepared by the following steps:

1. The synthesis process of MEPEs is shown in Figure 3.1. This process was developed

   by Higuchi et al.[36] in the previous work.

2. The resulting MEPE crystal was then added into DI-water. The concentration of the

   solution is 10 mg/mL.

3. The prepared inks was then immersed in ultrasonic bath for 30 mins to dissolve

   completely then form a true solution.

4. Filtrate the resulting inks before the printing process. The porous size of the filter

   membrane is 0.45 μm.

Figure 3.1 Synthesis process of MEPEs.[37]

3.1.3 Ink Deposition on Surfaces

Two substrates, ITO-glass and ITO-PEN, are ued in the following experiments. The wetting of ink on these substrates might have difference that the contact angle which is related to the dry drop diameter might also be different. So, the contact angle and the dry drop diameter have to be measured before the printing process.

The contact angle of inks on substrates is measured by the following steps:

1. Clean the substrates (3.0×4.0 cm^2) by rinsing sequentially with DI water and ethanol in ultrasonic bath, and dried in a vacuum oven.

2. Drip 5 μm of water on the substrates.

3. Take photograph by CCD camera.

4. Measure the contact angle with protractor

3.1.4 Printing of EC Thin Film

The coating of large-scale EC thin films have been produced in many other researches. In this section, we trying to print an EC thin film via inkjet printing process. Several analysis method were also taken to quantitatively describe the resulting thin film and also comparing to the other researches done previously. In inkjet printing process, all the patterns come from a single droplet initially. The morphology of the printed thin films are

highly related to the arrangement of these droplets. By adjusting the space between each droplet and the drying time between two layers, a condensed EC thin film with high uniformity can be obtained. The inkjet printer jetlab® 4 (MicorFab Technologies Inc., USA) was used in the experiments.

EC thin films are printed through the following steps:

1. Set the temperature of the moving plate at $40°C$.

2. Clean the ITO-PEN slides (3.0×4.0 cm^2) by rinsing sequentially with DI water and ethanol in ultrasonic bath, and dried in a vacuum oven.

3. Tuning the parameters of the electrical wave function which control the delivery of inks from inkjet nozzle to obtain stable droplets. The parameters used in this work are shown in Table 3.1. The droplet size is 77.5 μm in diameter.

Table 3.1 Inkjet printing parameters.

Rise Time (μs)	Dwell Time (μs)	Fall Time (μs)	Echo Time (μs)	Rise Time 2 (μs)	Idle Voltage (V)	Dwell Voltage (V)	Echo Voltage (V)
12	6	6	3	3	0	15	-45

4. The EC thin film was fabricated layer by layer. The first layer is an array of EC

   material. The printed space size between each droplet is 100 μm in both X-direction

   and Y-direction as shown in Figure 3.2.
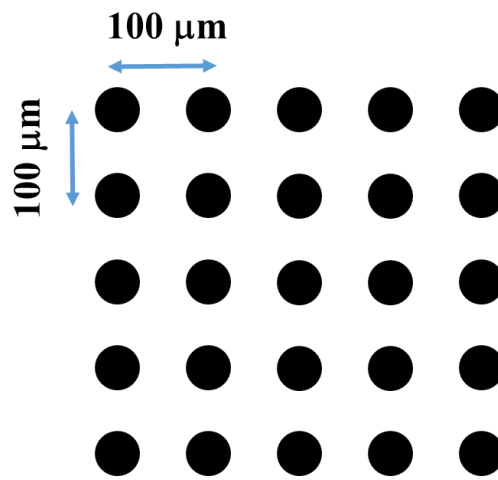
Figure 3.2 Array of the first printing scheme.

5. Repeat step.4 5 more times (6 times in total) to obtain EC thin film with condensed

   color.

6. Repeat step.4 then print the second array with different space size onto the first one.

   The second array have different space size between each droplet compare to the first

   one. The space size between droplets of the second array are 80 μm in X-direction

   and 125 μm in Y-direction as shown in Figure 3.3(a).

7. Print the third array that the space size between droplets are 60 μm in X-direction and

   160 μm in Y-direction as shown in Figure 3.3(b).

8. The array printed in step 4~6 are printed repeatedly with a rotate angle of 90 degrees.

Two EC thin films were presented after these steps and will be discussed later.
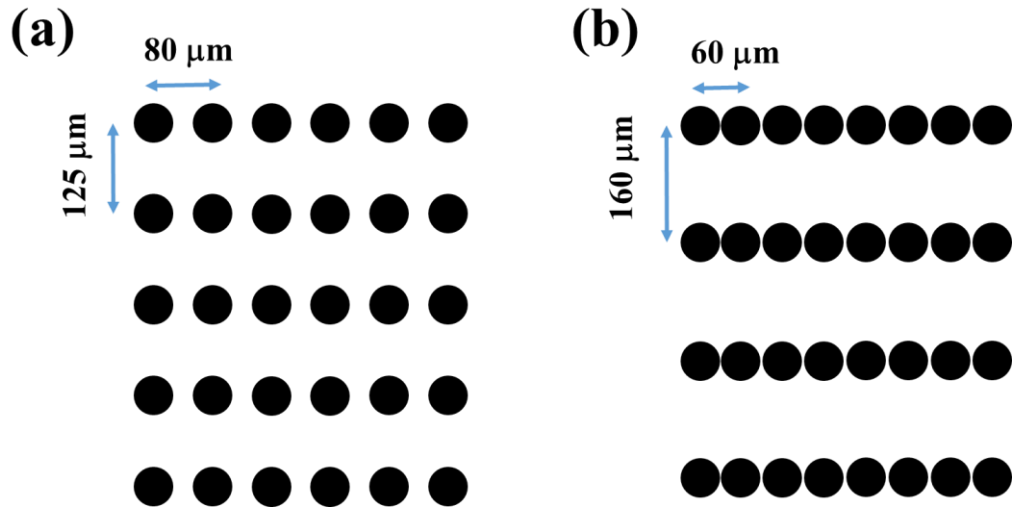
Figure 3.3 Arrays of the new printing scheme.

3.1.5 Solid-State Electrolyte

A transparent solid-state electrolyte thin film was prepared by mixing PVDF-HFP, EMIBTI, and acetone with a weight ratio of 1:4:7.[66]

The solid-state electrolyte thin film is prepared as following steps:

1. Add 1 g of PVDF-HFP into 7 g (8.85 mL) of acetone. Heating at $70^{\circ}C$ with stirring at 600 rpm until the polymer dissolved.

2. Add 4 g of EMIBTI into the resulting solution.

3. Pour the solution into a glass petri dish and dried in a vacuum oven at $70^{\circ}C$ for 24 h.

4. Peel off carefully and cut into proper size for ECD fabrication.

The resulting electrolyte film is shown in Figure 3.4.
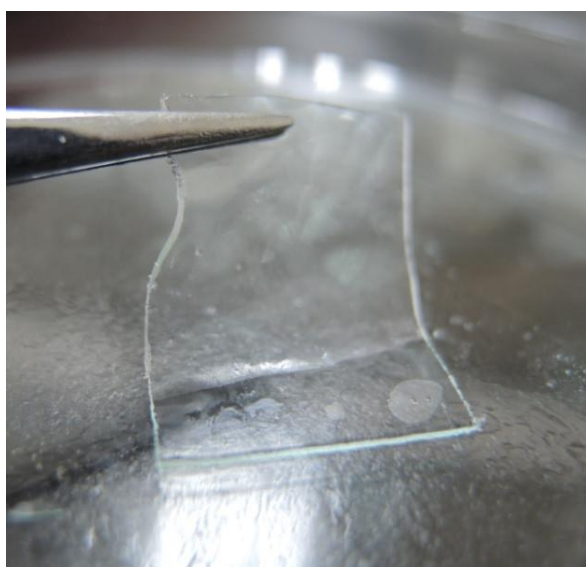
Figure 3.4 Solid-State Electrolyte.

3.1.6 Electrochromic Device

The EC devices were fabricated layer by layer as the structure shown in Figure 3.5.
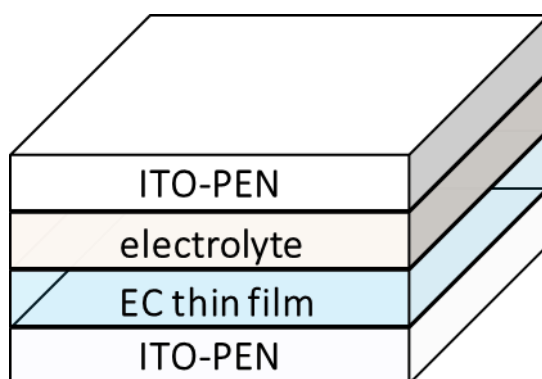
Figure 3.5 The layer by layer structure of the fabricated EC device.

These layers were assembled by the following steps:

1. Print MEPE thin films on ITO-PEN or ITO-glass substrates.

2. Cut the prepared solid-state electrolyte into a suitable size and then put it onto the

    prepared EC thin films.

3. Put on another layer of conductive transparent thin film.

3.2   Results & Discussion

3.2.1   Ink Deposition on Substrates

The contact angle of water on the two substrate were measured. The results are shown below (Figure 3.6):
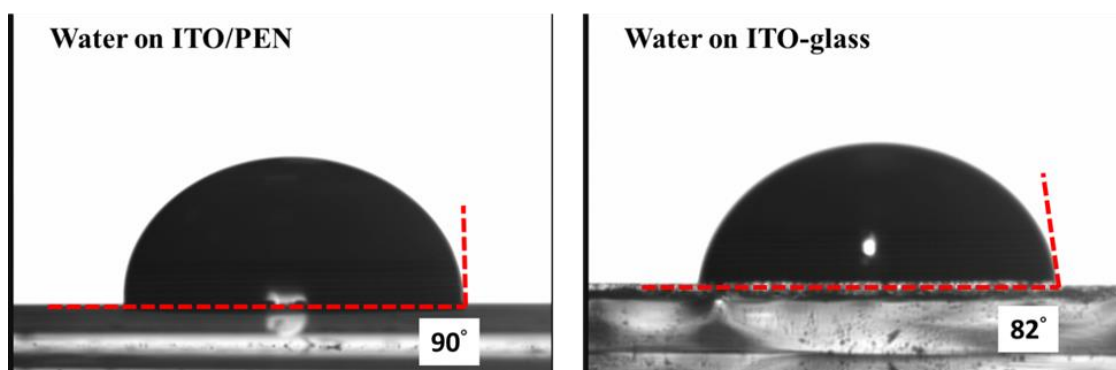
Figure 3.6 Water drop on two substrates

We find that the contact angles of water are 90° and 82° on ITO/PEN and ITO-glass respectively. These values don't have much difference between each other since both of the substrates were coated with ITO conductive layer. Besides contact angle, the dry drop diameter of the inks on two substrates were also measured. The inks were delivered in a row where the space size between each droplet is 100 μm. The optical images of the resuling dots are shown in Figure 3.7.
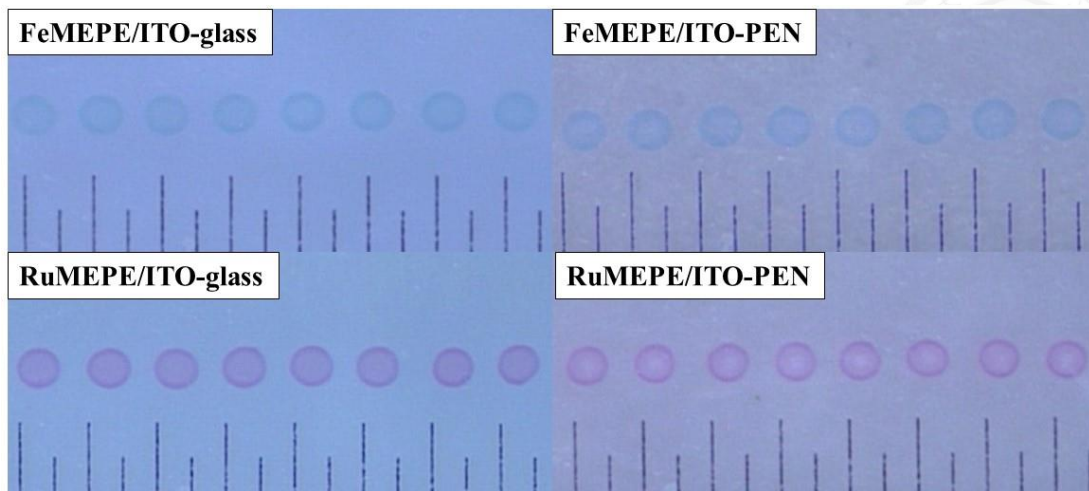
Figure 3.7 Dry drop morphology of two inks on substrates.

In Figure 3.7, EC material dots with high regularity can be observed. This result proofs the high stability of the inkjet printing process. The dry drop diameters can also be calculated in these images and the values are 70 μm and 60 μm on ITO-glass and ITO-PEN respectively. Because the contact angle of inks on ITO-PEN is slightly larger than that on ITO-glass, the dry drop diameter on ITO-PEN is smaller than that on ITO-glass. Although the dry drop diameters are different on these substrates, fabricating EC thin films via overlapping the dots can still be achieved since both of them are larger than the space size (> 50 μm). Due to these results, the same operating conditions can be used for the fabrication of EC materials on these two substrates
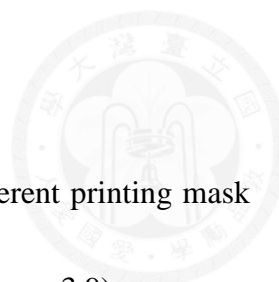
3.2.2 Influence of Printing Mask Scheme

In the previous section, two EC thin films were produced with different printing mask

scheme. The resulting EC thin films are shown below (Figure 3.8, Figure 3.9):
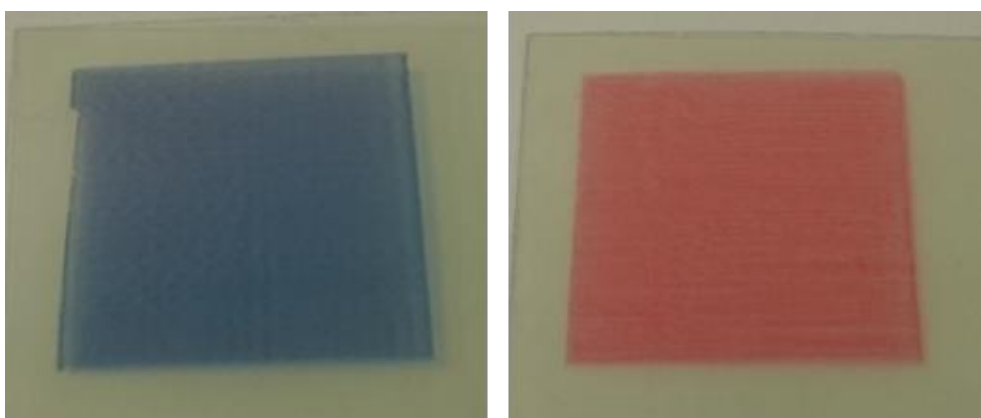
Figure 3.8 Morphology of the EC thin films printed by the first scheme.
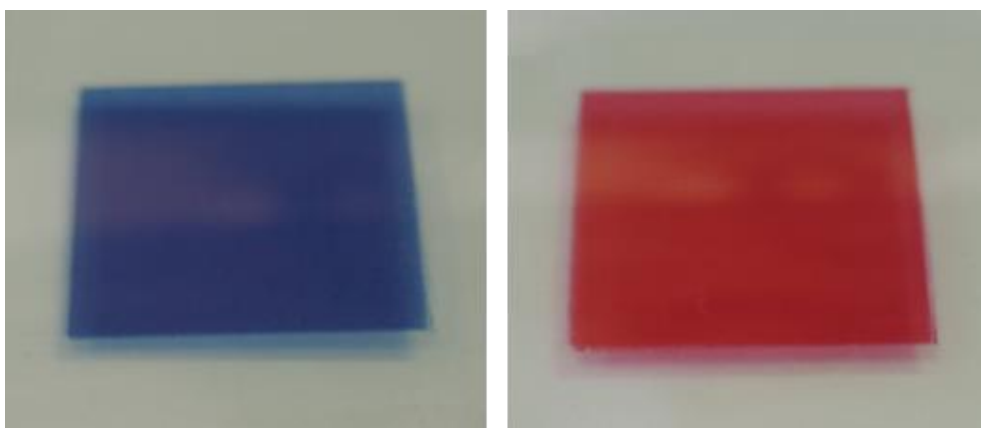
Figure 3.9 Morphology of the EC thin films printed by the new scheme.

In the first sample (Figure 3.8), the EC thin film were printed layer by layer with the same

array. The resulting EC thin film is not uniform that color change between dense and

sparse like mountains and valleys can be observed. A reasonable explanation for this

phenomenon is that when all layers were printed with the same array, the ink droplets will

deposit at same location repeatedly. This results in the mountains and valleys in the

printed EC thin film. The idea of this phenomenon is simulated as shown in Figure 3.10.

Assuming that a droplet is represented by a peak. After several times (four times) of

printing of the same array, the difference between mountains and valleys is emphasized

as it can be observed.
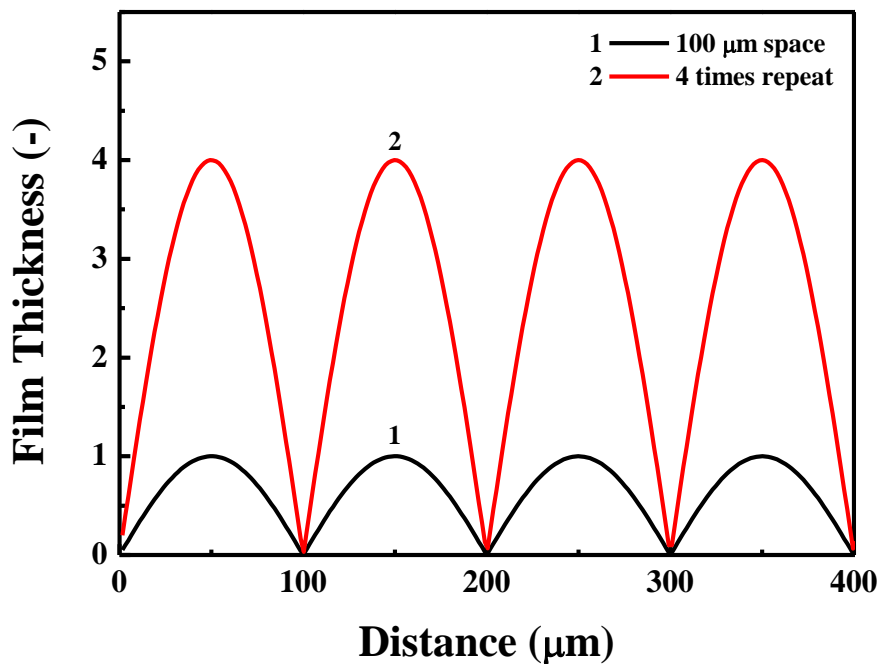
Figure 3.10 Illustration of the film thickness via printing same array repeatedly.

To avoid this problem, another masking scheme was proposed. The new masking scheme

is construct with several arrays that having same total dots but different arrangements within a specific area size as mentioned in the experimental section. The deposition of the droplets in these arrays and the superposition of them in x-direction are shown in Figure 3.11.
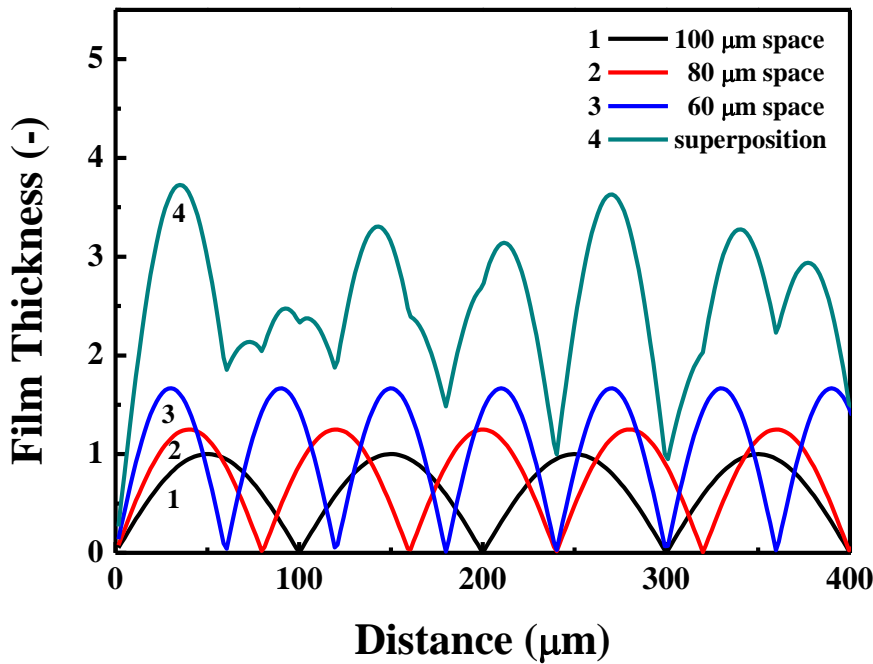
Figure 3.11 Illustration of the new masking scheme.

By the combination of these arrays with different droplet space size, the surface of the printed thin film (the resulting curve by superposition) becomes much smoother comparing to the previous one with the same total consumption of ink (same integral area of two curves) as shown in Figure 3.12. It can be found that the valleys observed in the first scheme are filled and the mountains are also erased in this new scheme so that an

uniform thin film can be successfully produced.
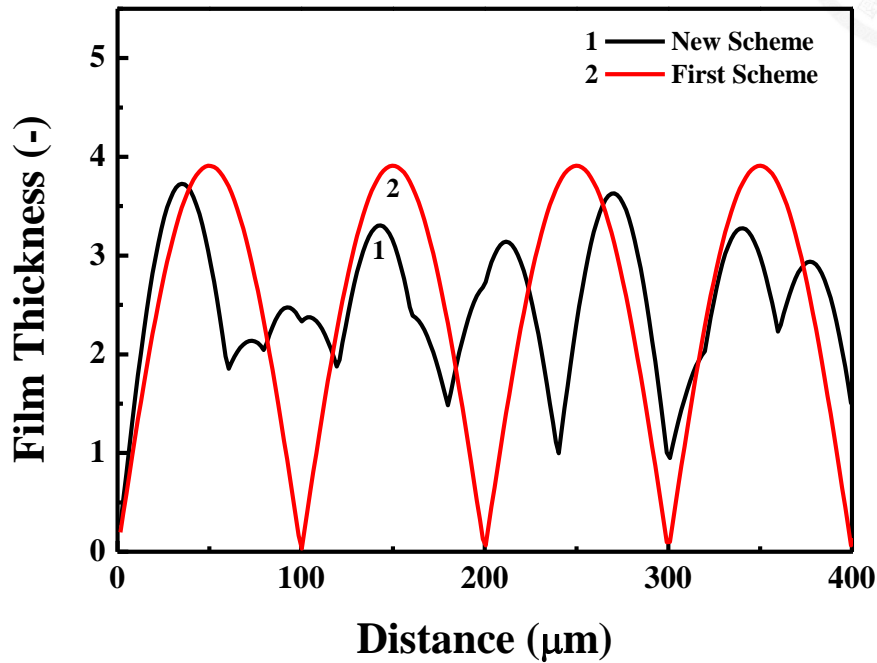
Figure 3.12 Comparison between two masking scheme.

The new masking scheme mentioned above only has effects in x-direction. This problem

can be easily resolved by rotating the masking scheme. To further comparing the EC thin

films produced by inkjet printing process with those produced by other coating method,

the following analyses are taken.

3.2.3 UV-vis Absorption

The UV-vis spectra of the printed EC thin films were measured to quantitavely describe the color of them. The In-situ UV-vis experiment was performed with a light source (DH-2000-BAL).
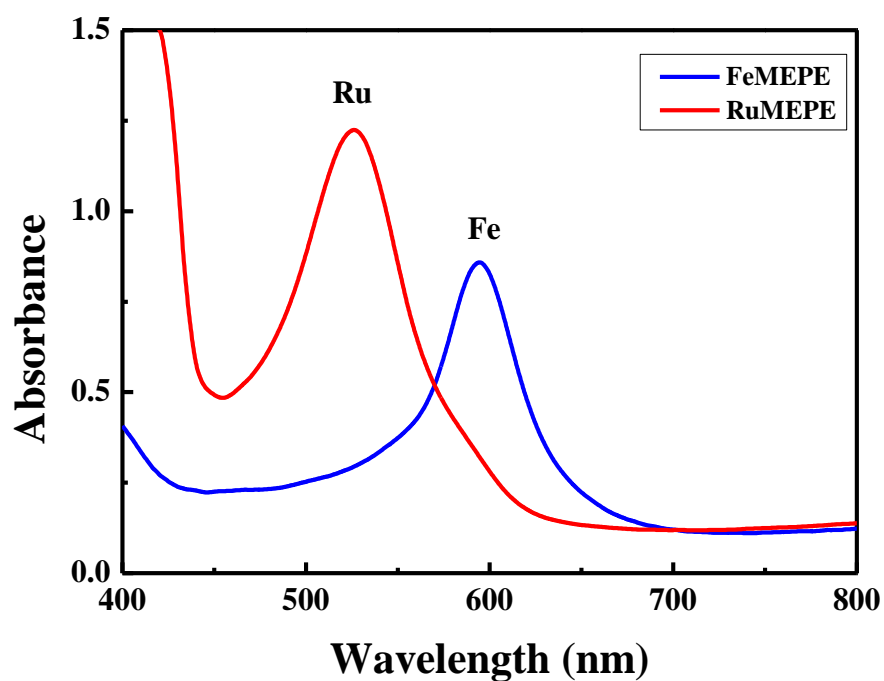
Figure 3.13 UV-vis absorption spectra of the printed EC thin films.
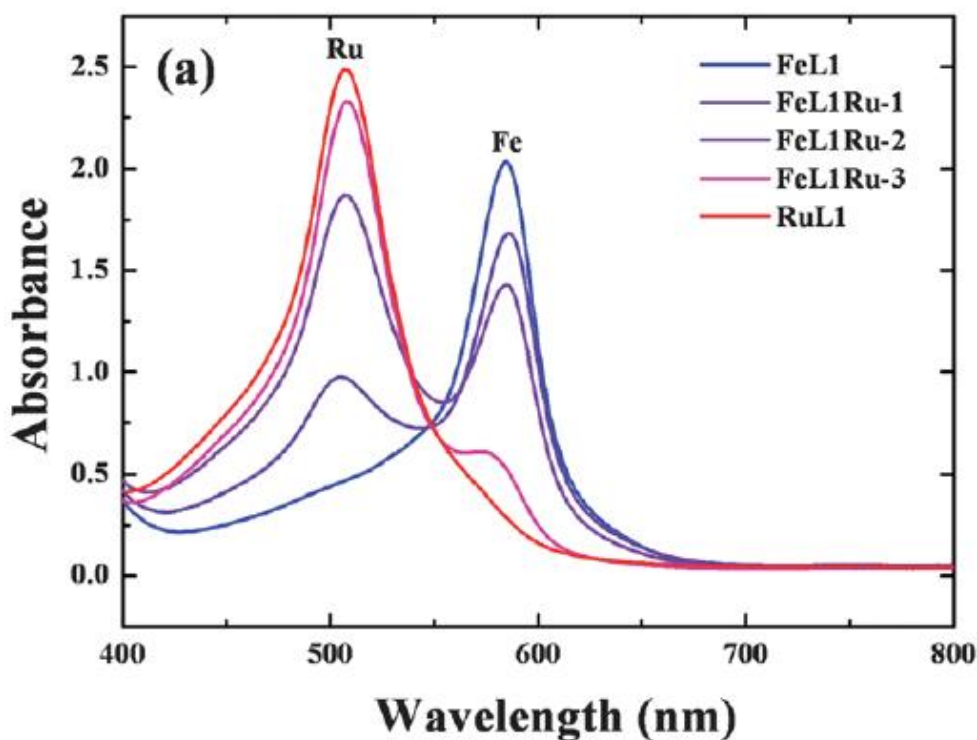
Figure 3.14 UV-vis absorption spectra produced in literature.[39]

Figure 3.13 shows the UV-vis absorption spectra of the printed EC thin films. The spectra

show absorption peaks at 515 nm and 580 nm for MLCT of Ru(II) and Fe(II) in MEPE

polymers, respectively. This result is in accordance to the previous research done by Hu

et al. via spray coating method as shown in Figure 3.14. The specific absorption peaks

have no change though the EC thin films are prepared from two different kinds of method.

The result in this experiment provides us the possibility of the further applications of this

metallo-supramolecular EC material via inkjet printing process.

3.2.4　Cyclic Voltammetry Method

CV-method is used to examine the electrochemical properties of the inkjet printed EC thin films. In this experiment, conductive substrate with EC thin films are served as working electrode, Pt-wire as counter electrode, and a home made Ag/Ag$^+$ electrode as reference. The EC thin film is submerged into 0.1 M LiClO$_4$/ACN electrolyte during this examination and the system settings are shown in Figure 3.15.
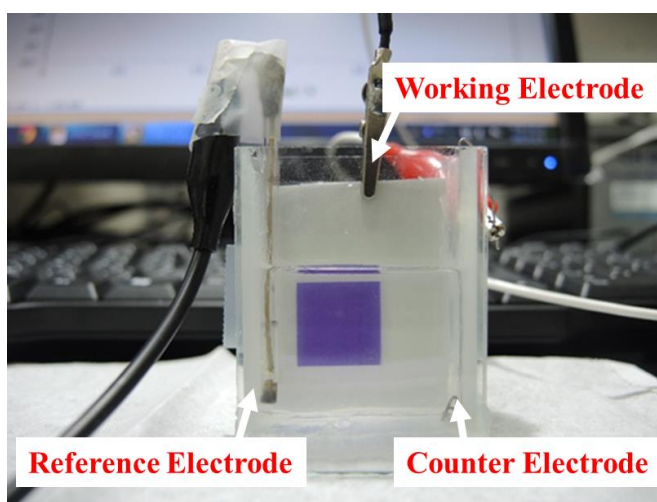
Figure 3.15 System setting of CV-method.

The electrochemical experiments were performed with a potentiostat (6271E, CH Instruments Inc., USA).
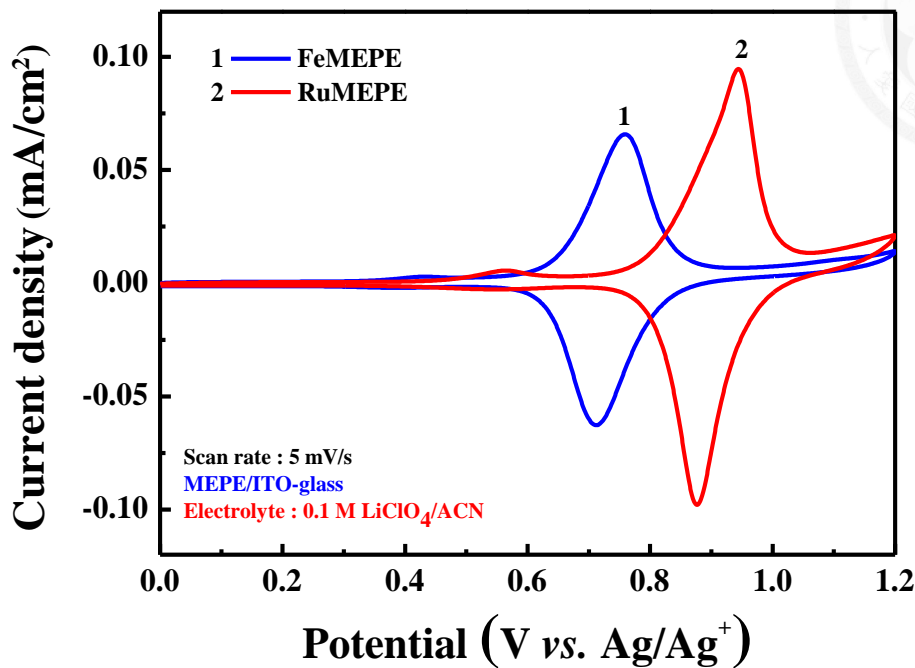
Figure 3.16 CV-diagram of the printed EC thin films.

Figure 3.16 shows the resulting CV-diagram of these printed EC thin films. A redox pair at 0.771 and 0.718 mV (vs. Ag/Ag$^+$) is observed at a scan rate of 5 mV s^{-1} for a Fe-MEPE thin film. These peaks refer to the electrochemical oxidation and reduction of Fe-MEPE respectively. Similarly, a redox pair for Ru-MEPE thin film associated with the color change can be seen at 0.961 and 0.896 mV (vs. Ag/Ag$^+$). These values are in accordance with the previous research and again providing us the possibility of the further applications of MEPEs via inkjet printing process.

3.2.5　Solid-State Electrolyte

The color change of the ECDs comes from the absorption change of the EC materials during redox reaction. Due to this reason, the electrolyte should be transparent or the fabricated ECD would not show the original color of the EC materials. The UV-vis absorption spectrum of the ionic liquid (EMIBTI) and the solid-state electorlyte made from it were both measured. The resulting spectrum are shown in Figure 3.17.
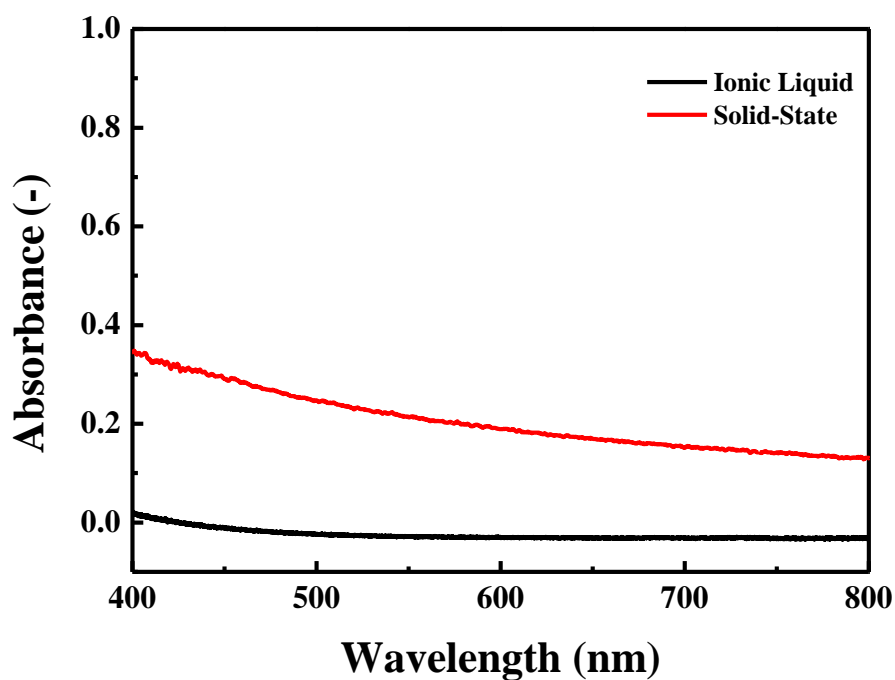
Figure 3.17 The UV-vis absorption spectrum of the solid-state electrolye.

Both of the absorption spectrum of the ionic liquid and the electrolyte are smooth. There is no peak in the range between 400 and 800 nm. The solid-state electrolyte shows highly transparency although the absorbance of it is higher than that of the pure ionic liquid.

The conductivity of the electrolyte is another important issue. The electrochemical impedance spectroscopy of the electrolyte was measured at the open circuit voltage with a perturbation voltage of 10 mV over the frequency range from 100 kHz to 0.1 Hz using Autolab PGSTAT30. Ionic conductivity(s) was calculated by the following equation:

$$\sigma = L/RA \qquad \textbf{(Eq. 3-1)}$$

where R is the bulk resistance of the electrolyte obtained from Nyquist plot, L is the thickness of electrolyte which was fixed by the 3M tape and Surlyn$^{\circledR}$ (DuPont, thickness~60 μm) between the ITO glasses, and A is the active area of the sample. (i.e., 1 cm2). By using $NaCl_{(aq)}$ (conductivity 12.9 mS/cm) as standard electrolyte, the overall resistence of the system can be eliminated. Then, the conductivity of the ionic liquid and the solid-state electrolyte are calculated to be 8.8 mS/cm and 8.6 mS/cm, respectively. We find that the conductivity of the solid-state electrolyte is only slightly decreased comparing to the ionic liquid.

3.2.6 Transmittance Change

The transmittance change at 580 nm in a inkjet printed FeMEPE film was investigated between 0 and 1.2 V (*vs*. Ag/Ag^{+}) with a switching time interval of 5 s. The dynamic transmittance curve was shown in Figure 3.18.
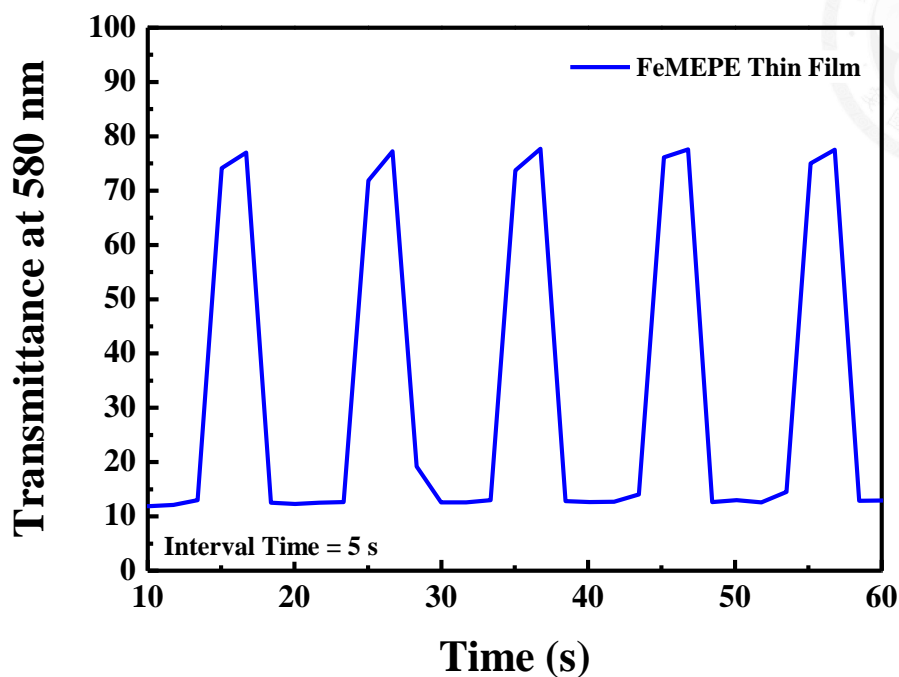
Figure 3.18 Transmittance change of Fe-MEPE film.

The printed EC thin film shows a high contrast as mentioned. The transmittance difference was calculated to be 65.5%. This value is in consist with previous research done via spray coating method. The bleaching time (t_b) and darkening time (t_d) can also be calculated from the dynamic transmittance curve (the time needed for 95% change of the saturated ΔT). The values of t_b and t_d for Fe-MEPE film are 2.0 s and 1.0 s, respectively. The prolong bleaching time (2.0 s) indicates that reduction of the central metal ligand is much faster than oxidation, because $Fe_{(II)}$ is more stable than $Fe_{(III)}$ in these MEPE complexes.
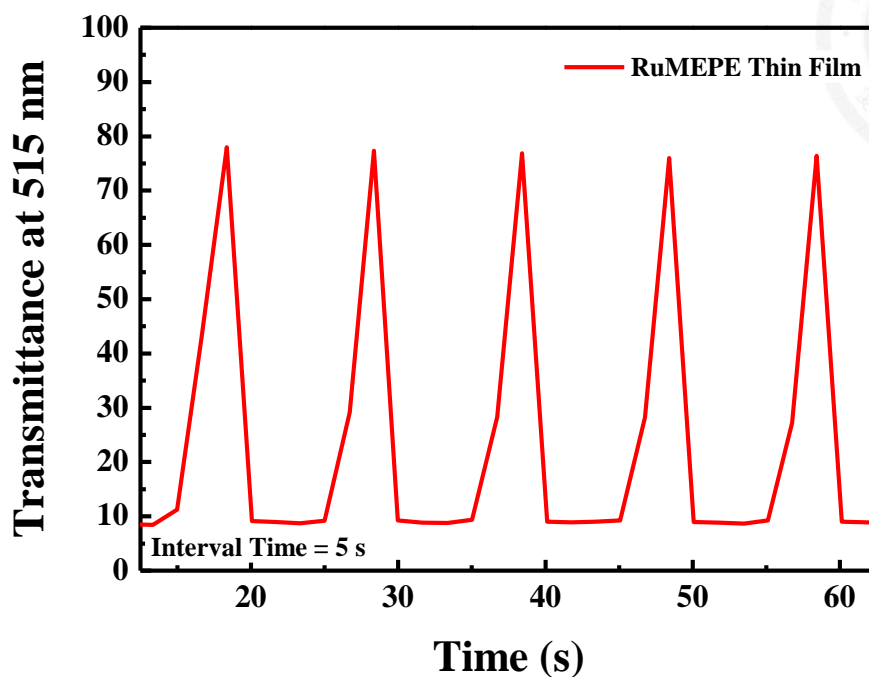
Figure 3.19 Transmittance change of Ru-MEPE film.

The Ru-MEPE film also shows similar characteristics as those of Fe-MEPE (Figure 3.19).

It shows a high contrast with a transmittance change (ΔT) of 68.6% at the characteristic

absorption wavelength of 515 nm. The values of t_b and t_d for Ru-MEPE film are 2.0 s and

1.0 s, respectively. Again, a prolong bleaching time (2.0 s) is represented for the same

reason that reduction of the central metal ligand is much faster than oxidation, because

$Ru_{(II)}$ is more stable than $Ru_{(III)}$ in these MEPE complexes.

The results of the inkjet printed thin films were discussed in the previous section and

the performance are in consist of those films prepared via spray coating. So, the

discussion will head to the ECD in this section. The printed ECD shows attractive EC

40

performance under either flat or bending conditions. Figure 3.20 shows the transmittance

changes of the fabricated devices between -3.0 and 3.0 V with a switching time interval

of 50 s.
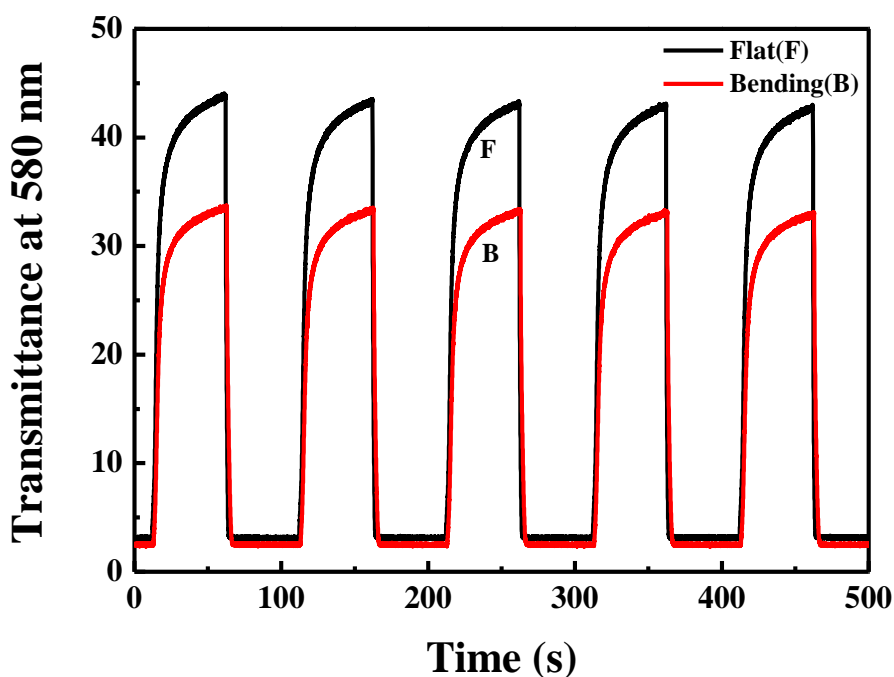
Figure 3.20 Transmittance change of Fe-MEPE device.

Under flat condition, the Fe-MEPE ECD shows a high contrast with a transmittance

change (ΔT) of 40.1% at the characteristic absorption wavelength of 580 nm. The color

change can be observed visually as shown in Figure 3.21(a). The values of t_b and t_d for

Fe-MEPE device at flat condition are 26 s and 2 s, respectively. The responsed time of

the ECD is much longer than that of the EC film. The only difference between them is

that different electrolyte were used. We find that the conductivity of the electrolyte is only slightly lower than the ionic liquid. This indicated that the prolong responsed time of the fabricated ECD is probably due to the contact problem between EC material and electrolyte and should be improved in the future. The electrochemical properties of the devices were also tested under bending condition with radius of curvature ~ 1.0 cm (Figure 3.21(b)).
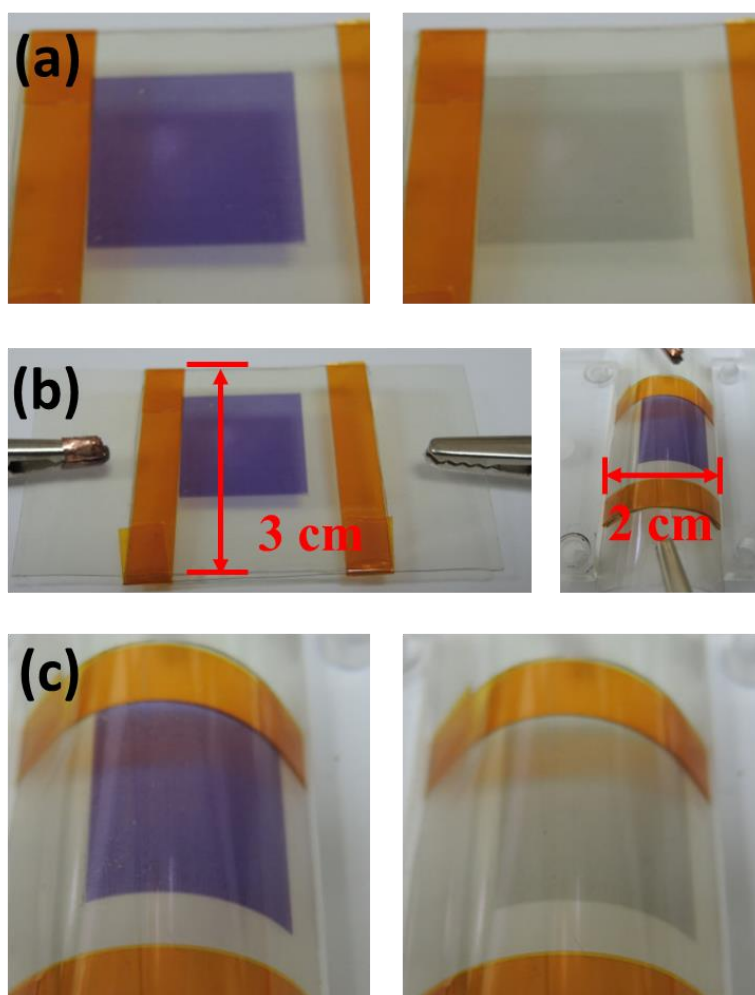
Figure 3.21 Color change of FeMEPE device.

The thickness of the ECD is 0.75 mm, and thus the ECD has an overall 7.5% strain after bending. The bent ECD can still exhibit a ΔT of 30.9% with observable color contrast (Figure 3.21(c)) upon darkening and bleaching, showing the strong mechanical stability of the ECD.

The Ru-MEPE ECD also shows similar characteristics as those of Fe-MEPE. Under flat condition, the Ru-MEPE ECD shows a high contrast with a transmittance change (ΔT) of 32.3% at the characteristic absorption wavelength of 515 nm. The color change can be observed visually as shown in Figure 3.23.
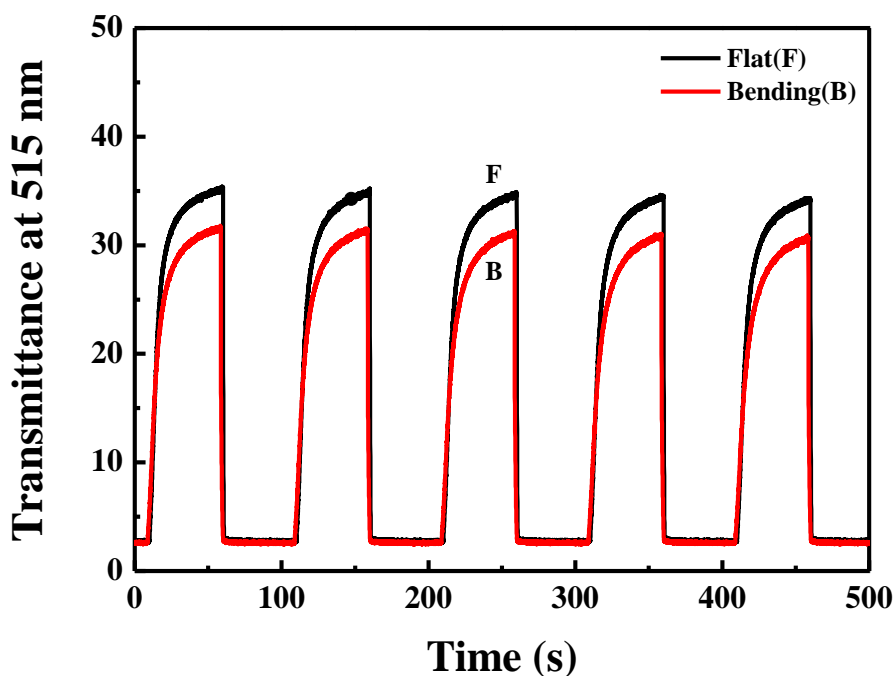
Figure 3.22 Transmittance change of the Ru-MEPE device.

The t_b and t_d can also be calculated from the dynamic transmittance curve. The values of t_b and t_d for Ru-MEPE device at flat condition are 27 s and 0.5 s, respectively. Again, a prolong bleaching time (27 s) is represented for the same reason that reduction of the central metal ligand is much faster than oxidation, because $Ru_{(II)}$ is more stable than $Ru_{(III)}$ in these MEPE complexes.
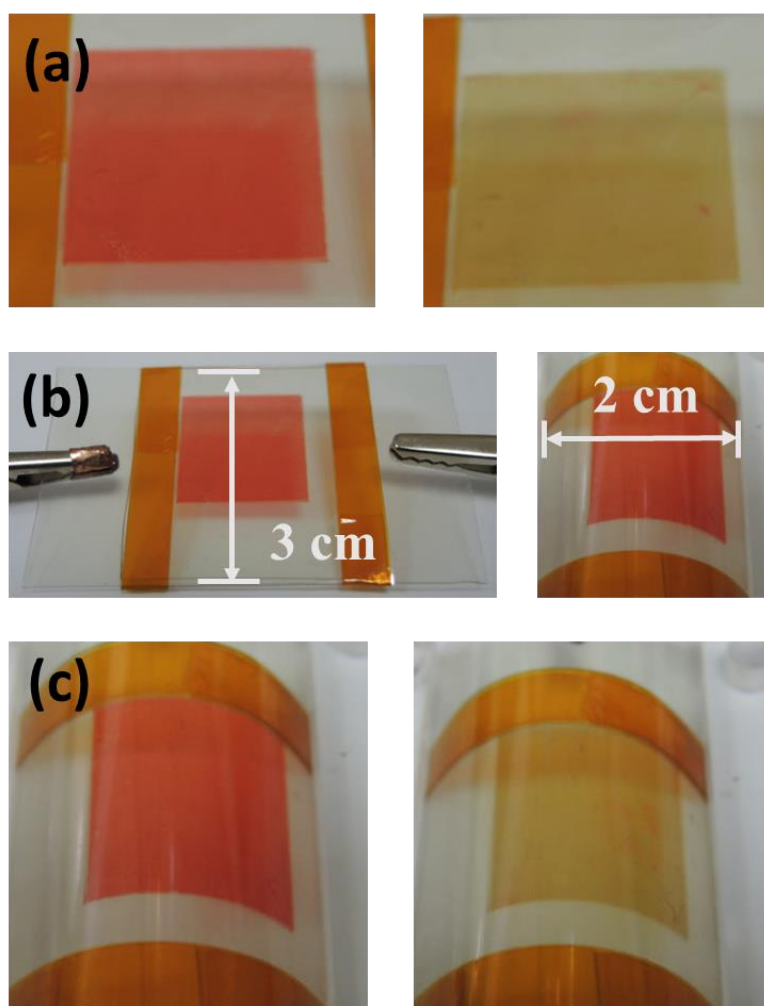

Figure 3.23 Color change of Ru-MEPE device.

3.2.7　Coloration Efficiency

The printed ECD also shows an impressive coloration efficiency, which is the extent of optical density change caused by a fixed charge/discharge amount during redox reaction of an EC material. Coloration efficiency can be calculated from the following equation:

$$\eta = \log\frac{T_b}{T_c}/Q_d \qquad\qquad \textbf{(Eq. 3-2)}$$

Where η (cm^2 C^{-1}) is the coloration efficiency, T_b and T_c are the bleached and colored transmittance values, respectively, and Q_d is the injected/ejected charge per unit area. The current change was recorded simultaneously with the transmittance change experiment. Figure 3.24 shows the charge/discharge amount for a Fe-MEPE ECD under flat and bending conditions.

Figure 3.24 I-t curve of the FeMEPE device during transmittance change.

F:2.86 mC/cm^2

B:2.98 mC/cm^2
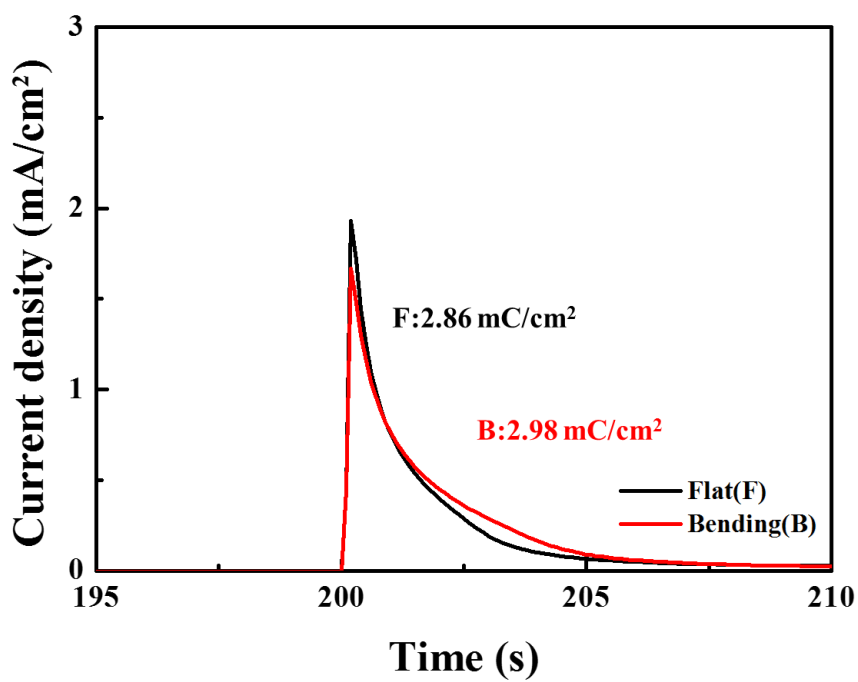
Figure 3.25 Enlarged part of the oxidation peaks of FeMEPE device.
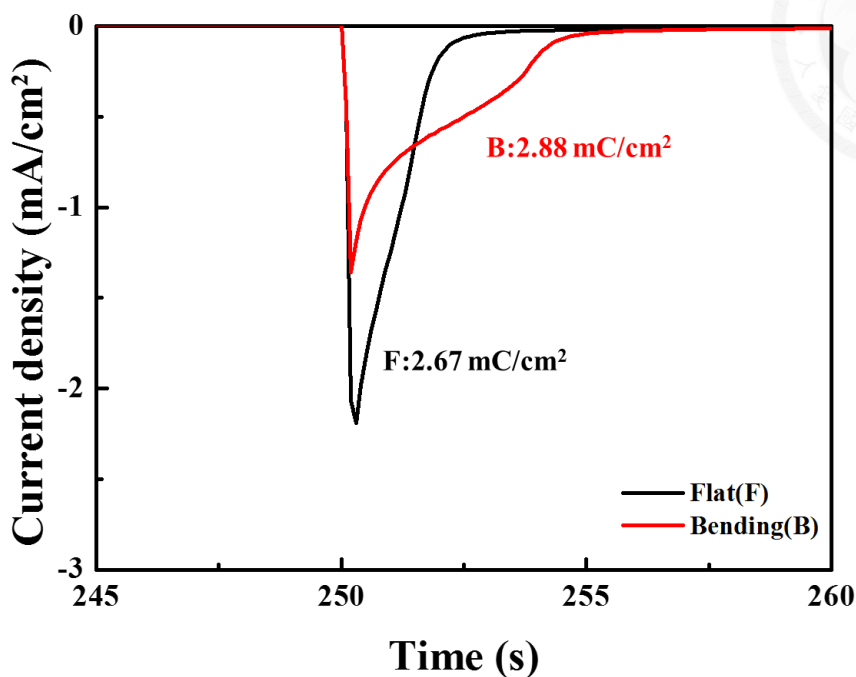
Figure 3.26 Enlarged part of the reduction peaks of FeMEPE device.

From the oxidation peaks (Figure 3.25), which show the charge amount to bleach a flat

ECD after switching the applied voltage from -3.0 V to 3.0 V, the value of Q_d of 2.86

mC/cm^2 can be obtained. Similarly, the amount of charge to darken the flat ECD can be

calculated from the reduction peaks (Figure 3.26) as 2.67 mC/cm^2. The coloration

efficiency can then be calculated as 445 cm^{2}C^{-1} by inserting the later value into equation

(1). Under bending conditions, Q_d slightly increases by ~10% compared to the flat one,

and therefore 2.98 mC/cm^2 for bleaching and 2.88 mC/cm^2 for darkening were obtained.

This suggests more leakage currents were noticed in the bent ECD. In addition, bending

also leads to a lower transmittance difference (30.1%, Table 3.2). These lead to the

coloration efficiency of the bent ECD is 381 cm^{2}C^{-1}, which is 15% lower than that under flat condition, nevertheless, but the value is still quite impressive for regular ECDs.

The current change of the RuMEPE device were also recorded and the results are shown in Figure 3.27. From the oxidation peaks (Figure 3.28) the value of Q_d of 2.77 mC/cm^2 can be obtained. Similarly, the amount of charge to darken the flat ECD can be calculated from the reduction peaks (Figure 3.29) as 2.10 mC/cm^2. The coloration efficiency can then be calculated as 521 cm^{2}C^{-1}. Under bending conditions, Q_d of 2.83 mC/cm^2 for bleaching and 2.46 mC/cm^2 for darkening were obtained. Bending of the RuMEPE device also leads to a lower transmittance difference (29.9%). These lead to the coloration efficiency of the bent ECD is 439 cm^{2}C^{-1}.
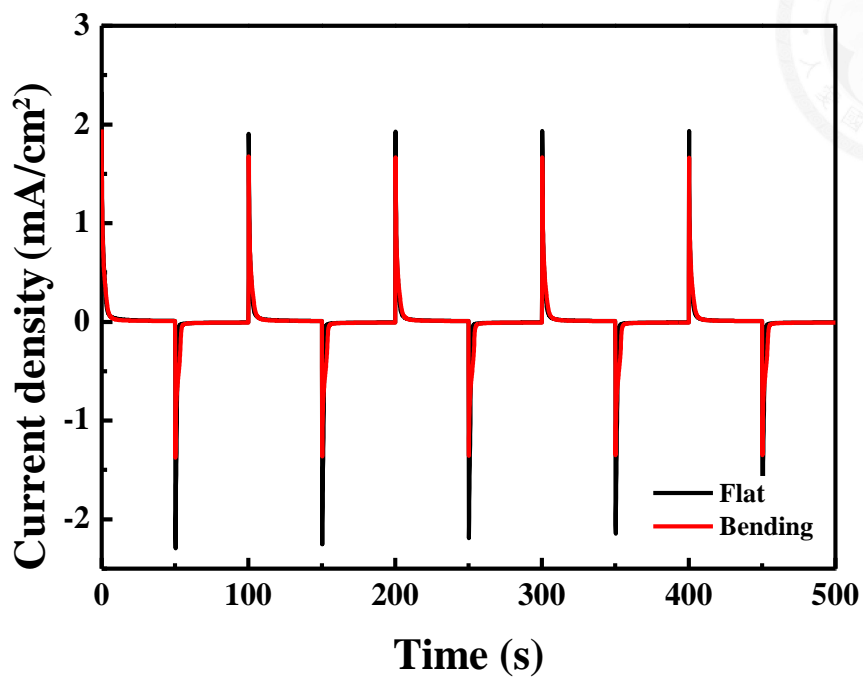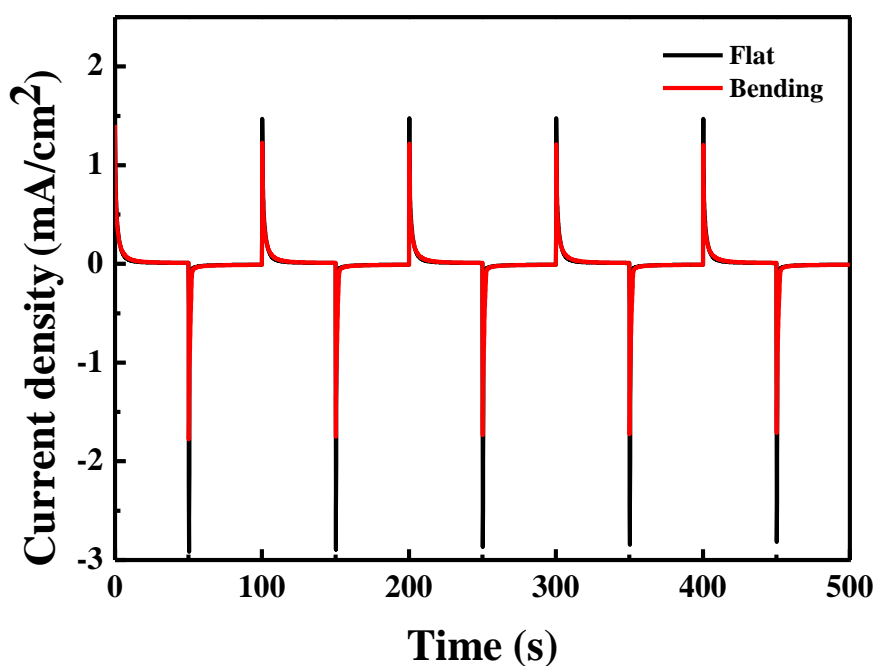

Figure 3.27 I-t curve of the RuMEPE device during transmittance change.
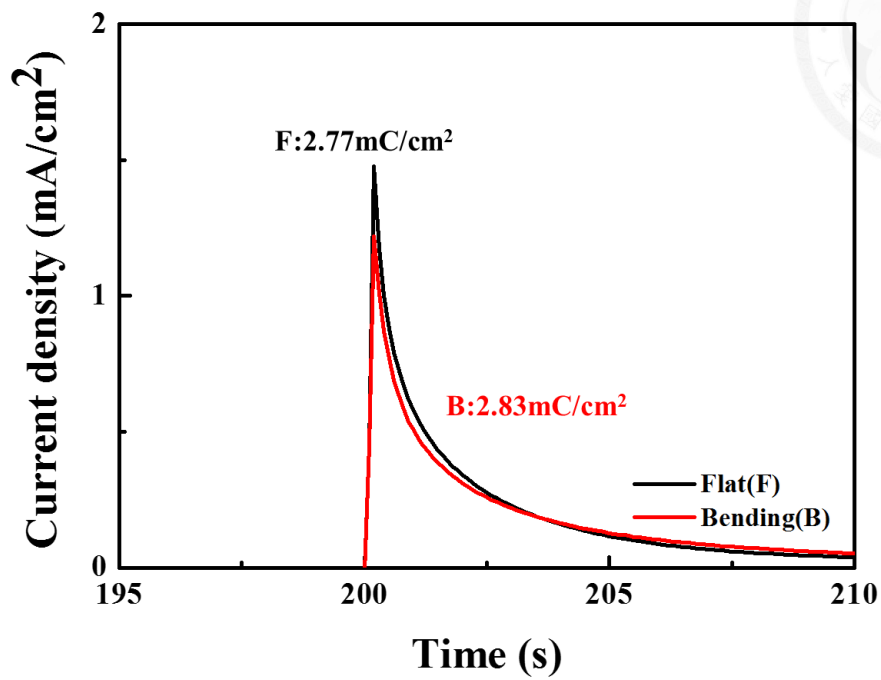
Figure 3.28 Enlarged part of the oxidation peaks of RuMEPE device.
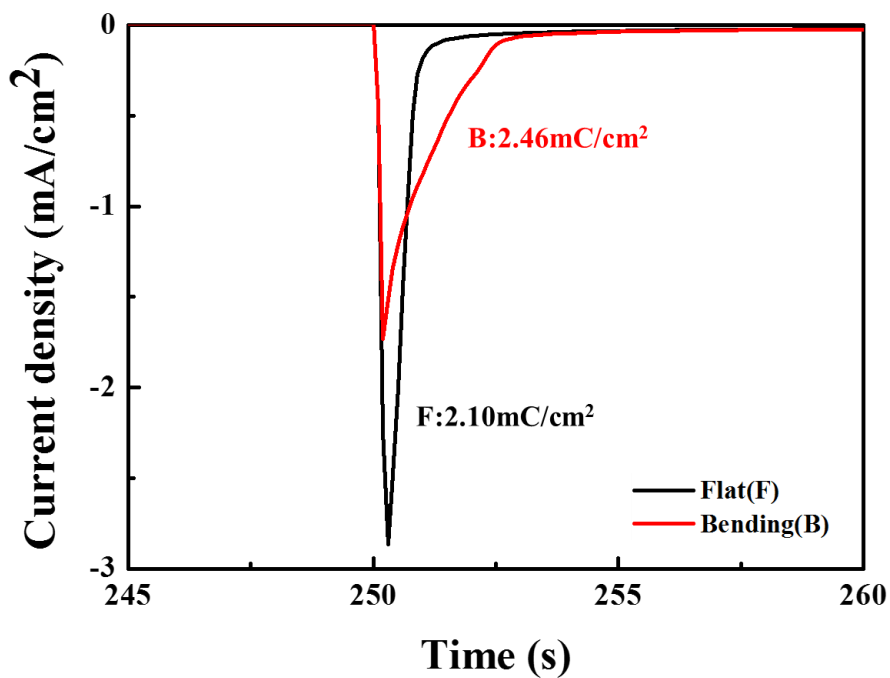
Figure 3.29 Enlarged part of the reduction peaks of RuMEPE device.

Table 3.2 The EC properties of single color flexible ECDs[*]

Device	Max wavelength change (λ_{max}, nm)	Darkening time (t_d, s)	Bleaching time (t_b, s)	Transmittance change (ΔT, %)	Charge/discharge amount (Q, mC cm^{-2})	Coloration efficiency (η, cm^2 C^{-1})
FeMEPE	580	2.0	26	40.1	2.67/2.86	445
Fe Bending	580	2.0	21	30.1	2.88/2.98	381
RuMEPE	515	0.5	27	32.3	2.10/2.77	521
Ru Bending	515	2.0	21	29.9	2.46/2.83	439

[*] The color of the printed ECD was switched between -3.0 and 3.0 V with a time interval of 50 s.

3.2.8 Long-Term Stability

The stability is an important issue in the study of an ECD. Figure 3.30 shows the

transmittance changes of the fabricated devices between -3.0 and 3.0 V with a switching

time interval of 50 s.
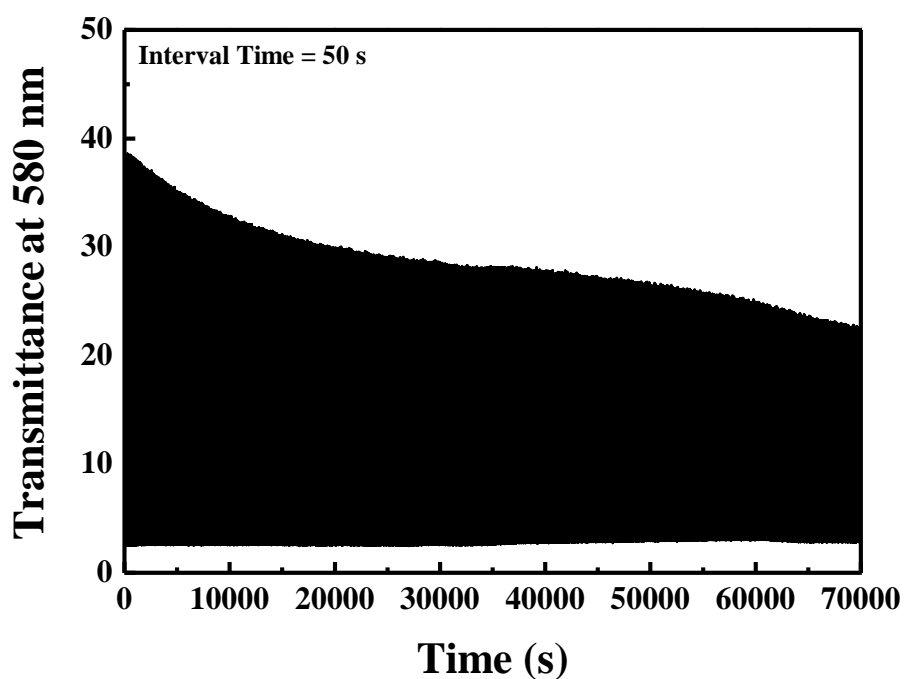
Figure 3.30 Long-term transmittance change of the Fe-MEPE device.

After 700 cycles of redox reaction, the contrast decreased that it shows transmittance

change (ΔT) of 20% which is only one half of the original value. This stability test shows

that, the bleach state is not stable when using EMIBTI as electrolyte and without charge

storage layer.

Chapter 4 Multi-Color EC device
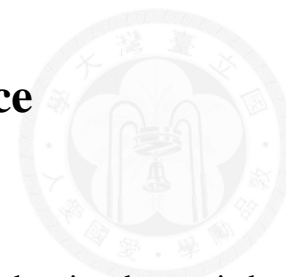
To produce a variety of color possibilities for EC materials, chemists have tried various chemical synthetic methods, such as side chain functionalization and copolymerization. Besides polymer synthesis, one can also utilize the ligand/ion interactions in coordinated polymers to synthesis EC materials with different absorptions. In this chapter, EC materials in two different colors were mixed together in various ratios via inkjet printing process and the electrochemical properties of these printed EC thin films will also be discussed.

4.1 Experimental

4.1.1 Color Mixing Serious

To demonstrate the feasibility of printing multi-color thin film patterns with the least consumption of inks, the dot ratio between red Ru-MEPE and blue Fe-MEPE inks are adjusted digitally to give sequential color variations from red, purple to blue. The color mixing EC thin films were prepared by the following steps:

1. Set the temperature of the moving plate at 40°C.

2. Clean the ITO-glass slides (3.0×4.0 cm^2) by rinsing sequentially with DI water and

ethanol in ultrasonic bath (DELTA DC300H), and dried in a vacuum oven.

3. The droplet parameters are the same as described in previous chapter. The droplet size is 77.5 μm in diameter.

4. Print a series of arrays of Fe-MEPE. The masking scheme is the blue dots shown in Figure.X. The space size between each droplet is 50 μm.

5. Print another series of array. The masking scheme is the red dots shown in Figure 4.1.

6. Repeat step.4 and step.5 for 3 more times (total 4 times) to acquire condensed thin film.
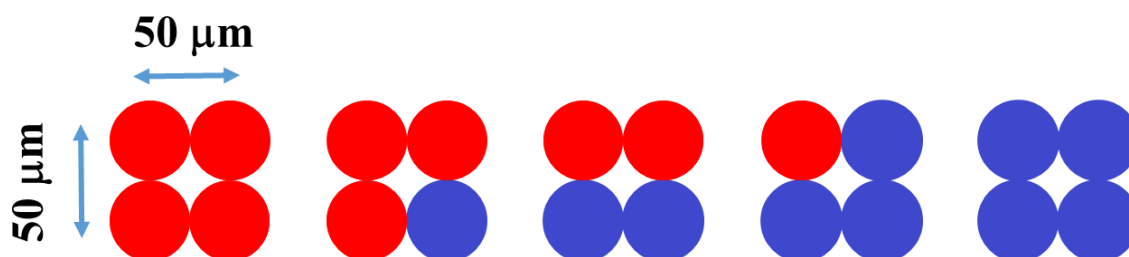
Figure 4.1 Masking scheme of color mixing series.

4.1.2   Multi-Color EC Pattern

In inkjet printing process, the most attractive thing is that thin film patterns can be produced without any mask requirement. In this section, an EC thin film with multi-color pattern is fabricated to demonstrate the ability of precise deposition for the inkjet printing process. The multi-color EC thin film pattern was prepared by the following steps:

1. Set the temperature of the moving plate at 40°C.

2. Clean the ITO-glass slides (3.0×4.0 cm^2) by rinsing sequentially with DI water and ethanol in ultrasonic bath (DELTA DC300H), and dried in a vacuum oven.

3. Print EC thin film pattern which the "NTU" letters are in blank sites as shown in Figure 4.2 with RuMEPE ink.

4. Print another EC thin film pattern which is complementary to the previous one as shown in Figure 4.3 with FeMEPE ink.

Figure 4.2 Pattern with "NTU" letters in blank sites.

Figure 4.3 Pattern complementary to the previous one.

4.1.3   Electrochromic Device

The fabrication of the multi-color EC devices were achieved by the procedure described in the previous chapter.

4.2   Results & Discussion

4.2.1   Color Mixing Series

A series of drop arrays with different red/blue printing ratios were printed in the

color masking scheme shown in Figure 4.1. to produce squares of 1.0 cm^2 on ITO-glass.

The resulting color mixing EC thin films are shown in Figure 4.4.
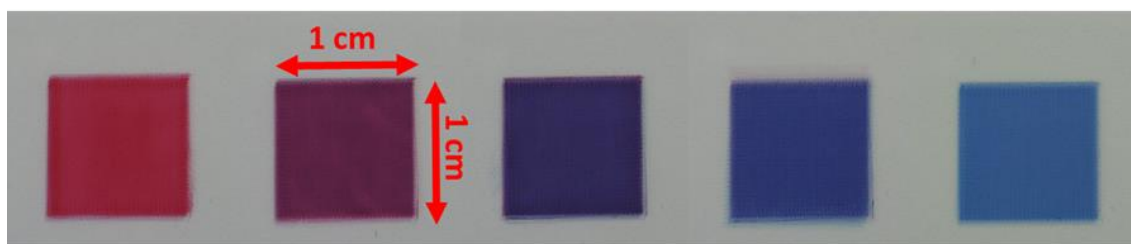
Figure 4.4 Color mixing EC thin films produced by inkjet printing.

These EC thin films have various color in series as proposed in our color masking scheme.

The arrangement of the printed EC dots in two different colors can clearly be seen under

optical microscope (Figure 4.5).
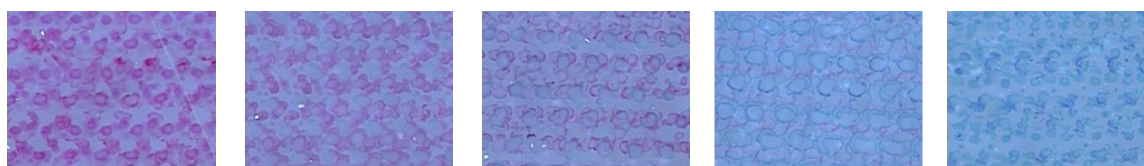
Figure 4.5 Arrangement of the droplets under optical microscope.

4.2.2 Multi-Color EC Pattern

Besides the color mixing series, the multi-color patterning EC thin films were also fabricated as shown in Figure 4.6.

Figure 4.6 Multi-color EC thin film patterns.

In this experiment, the masking schemes were loaded into the printing program from bitmap files which can be easily designed via basic graphics software. First, an EC thin film with the blank "NTU" letters was printed with the red Ru-MEPE ink as shown in Figure 4.6(a). Then, another masking scheme was used with the blue Fe-MEPE ink to produce EC thin film as shown in Figure 4.6(b). These EC thin films deposit precisely at the location where they were designed, hence the blank and blue "NTU" letters can be observed. Since the masking schemes were complementary to each other, we can print them together with two kinds of ink. These two patterns can be printed together and perfectly merged into one multi-color pattern as shown in Figure 4.6(c).

4.2.3 UV-vis Absorption

To quantitatively describe the relationship between the dot ratios of two inks and the color of the resulting EC thin films, the UV-vis adsorption spectra were measured and results were shown in Figure 4.7.
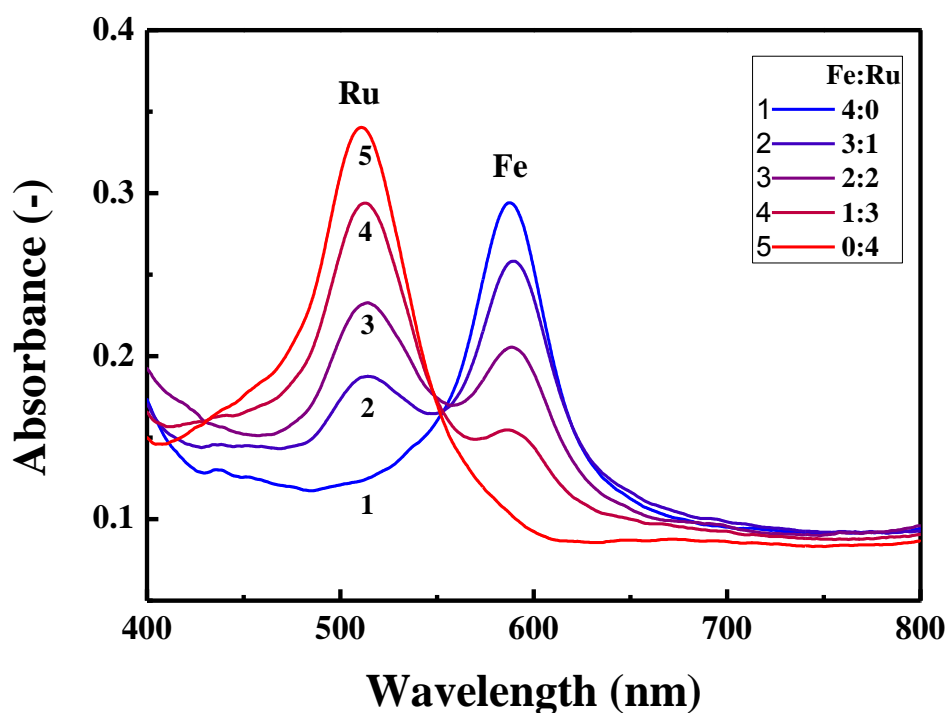
Figure 4.7 UV-vis absorption spectra of color mixing series.

The absorbance at 515 nm due to the MLCT of Ru(II) is proportional to the quantity of Ru-MEPE ink in the fabricated EC thin films. The same phenomenon is also observed at 580nm, where the absorbance is also proportional to the quantity of printed Fe-MEPE ink.

4.2.4   Cyclic Voltammetry Method

The CV-method were also used to study the electrochemical properties of the color

mixing EC thin film. The resulting CV-diagram is shown in Figure 4.8.
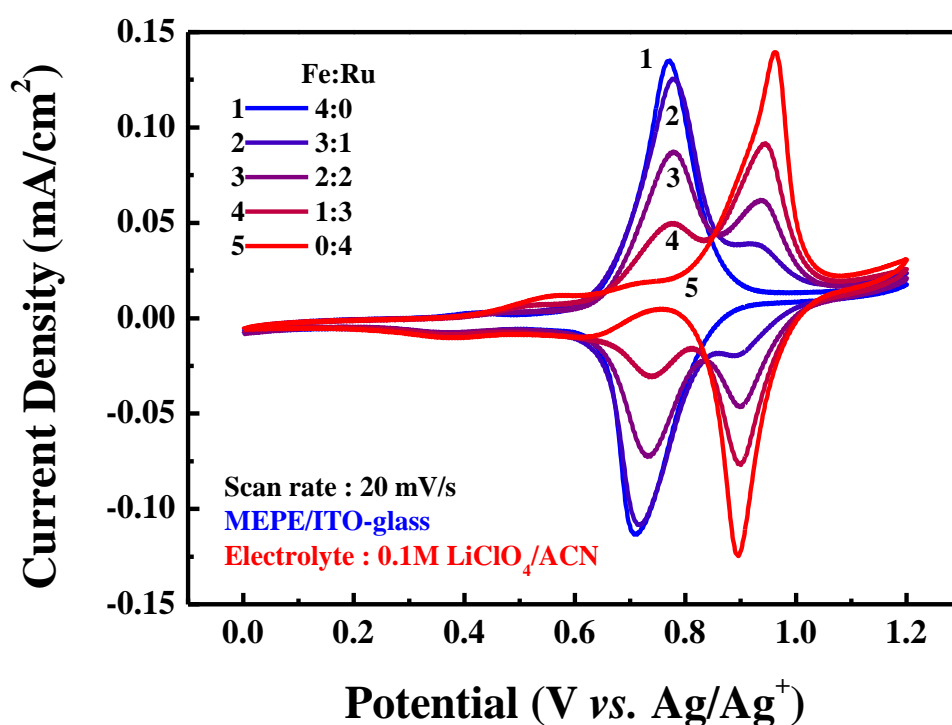
Figure 4.8 CV-diagram of the inkjet printing color mixing EC thin films.

For printed thin films containing both Fe-MEPE and Ru-MEPE, two redox pairs can

be observed almost at the same potentials noticed for pure Ru-MEPE and Fe-MEPE thin

films. Similar color mixing can also be achieved via synthesis process in previous

study.[39] However, the redox pairs of the synthesized mixed-color polymers showed

larger peak shifts in potentials. In this work, the redox peaks of color mixing samples

show negligible potential shifts (< 10 mV) compared with those of color mixing EC thin films via synthesis process (> 20 mV). The negligible potential shifts indicate a fairly weak ligand interaction with the central metal ions, simply because the color mixing is achieved physically by stacking ink drops instead of metal alternating chemical synthesis. This advantageous physical stacking characteristic can be used to control color variation by tuning the supplied voltage and will be discussed in the following section.

Table 4.1 Oxidative and reductive peak potentials for the pure and mixing thin films.

	E_{ox} of Fe^{2+}(mV)	E_{red} of Fe^{2+}(mV)	E_{ox} of Ru^{2+}(mV)	E_{red} of Ru^{2+}(mV)
FeMEPE	771	718	—	—
Fe/Ru = 3:1	777	718	931	899
Fe/Ru = 2:2	778	719	936	898
Fe/Ru = 1:3	780	719	940	895
RuMEPE	—	—	963	896

Table 4.2 Oxidative and reductive peak potentials for the synthesized thin film.[39]

	E_{ox} of Fe^{2+} (mV)	E_{red} of Fe^{2+} (mV)	E_{ox} of Ru^{2+} (mV)	E_{red} of Ru^{2+} (mV)
FeL1	768	741	—	—
FeL1Ru-1	773	744	922	903
FeL1Ru-2	781	746	933	904
FeL1Ru-3	785	753	945	909
RuL1	—	—	949	916

4.2.5 Multi-Color EC Devices

The printed ECD can exhibit multiple colors by manipulating the printed patterns or the applied electrical signals. UV-vis absorption spectra of the ECD fabricated with the color mixing sample were measured under various potential. The sample being discussed in this section have dots ratio of 2:2 between FeMEPE and RuMEPE.

After bleached under 3.0 V for 30 s, the ECD is then darkened at various reduction voltages while the UV-vis absorption spectra were recorded (Figure 4.9).
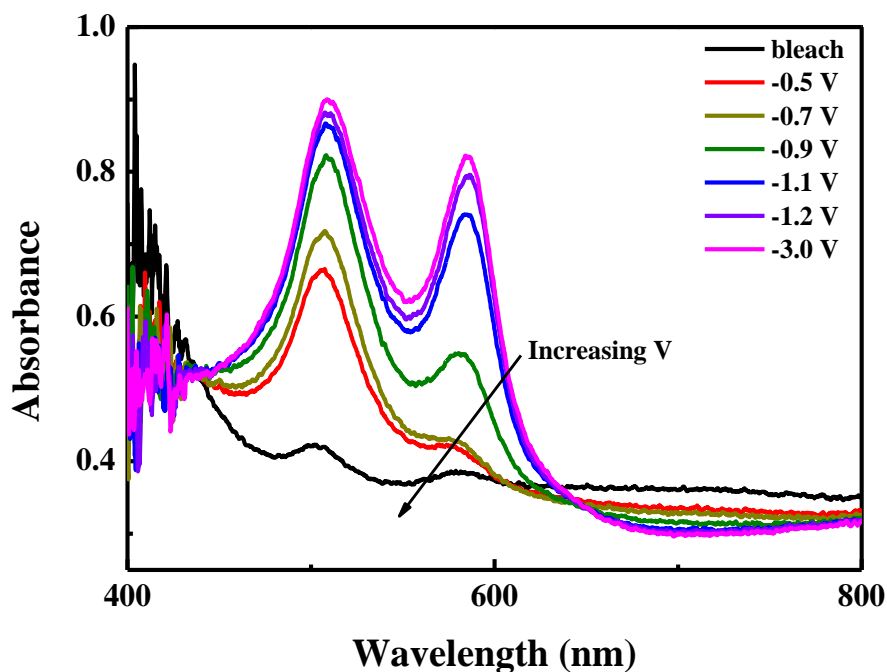
Figure 4.9 UV-vis absorption spectra of sample2:2 at different potential.
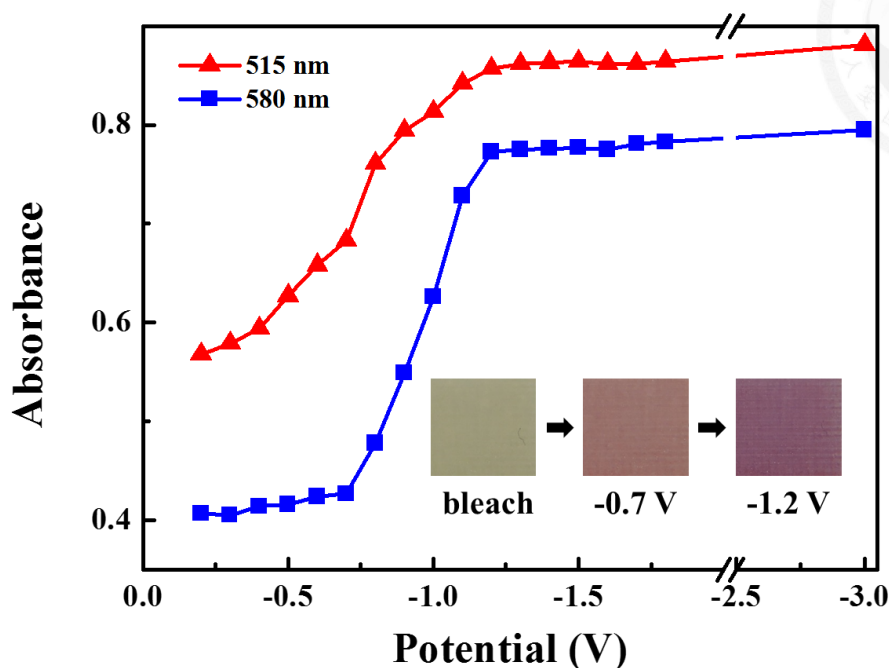
Figure 4.10 Absorbance change with different potential at specific wavelength.

Because of the difference in redox potential, the Ru(III) was reduced earlier than Fe(III) did so that the ECD shows red color initially at relatively higher applied potential. As shown in Figure 4.10, the absorbance of this sample at 515 nm gradually increased along with the decreasing of applied potential. The absorbance at 580 nm remains nearly unchanged while the potential is higher than -0.7 V. After the applied potential is reached lower than -0.9 V, Fe(III) in Fe-MEPE can be reduced so that the absorbance at 580 nm starts to rise and the blue color starts to show up. As summarized in Figure 4.10, the absorbance of this sample at 515 nm and 580 nm both reach a plateau and the color

become purple when a potential lower than -1.2 V is applied, indicating complete

reduction of both Fe(III) and Ru(III) in the ECD. Due to the high electrochemical stability

of these MEPE polymers, the color of this ECD remains unchanged even when a voltage

as low as -3.0 V is applied.

Another flexible EC device fabricated with the multi-color patterning was also

produced in this section. The color change of this ECD is also examined under various

applied potential and found out to have three different color states as shown in Figure

4.11.
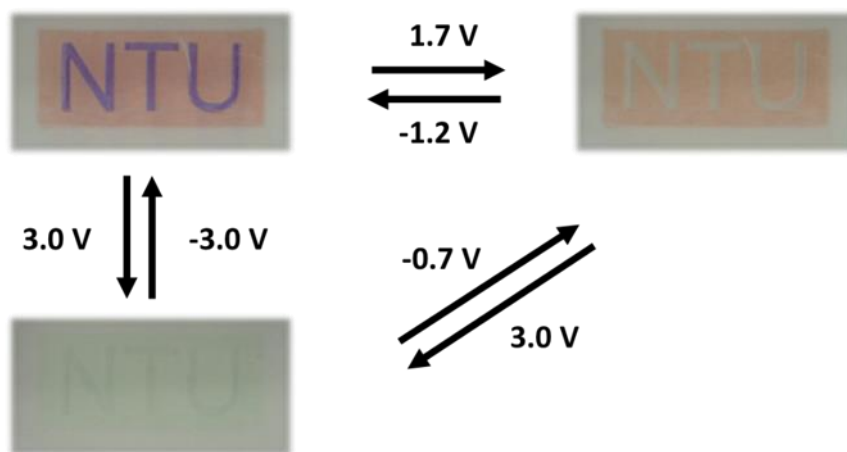
Figure 4.11 Color states of the patterned ECD at flat condition.

Since the blue Fe-MEPE can be oxidized more easily than the red Ru-MEPE, the blue

pattern can be bleached with red surrounding pattern unchanged. To completely bleach

the ECD, a voltage of 2.0 V is required. While recovering the color patterns, the red one

still shows a faster response at low voltages and both colors are recovered at -2.0V. The

same phenomenon was also observed in the previous section where red color appears

earlier than blue color does. This indicate that the redox potentials of these MEPEs remain

unchanged after mixing via inkjet printing process. Moreover, the ECD shows great

mechanical stability and exhibits the same color display even under bending conditions

(Figure 4.12).
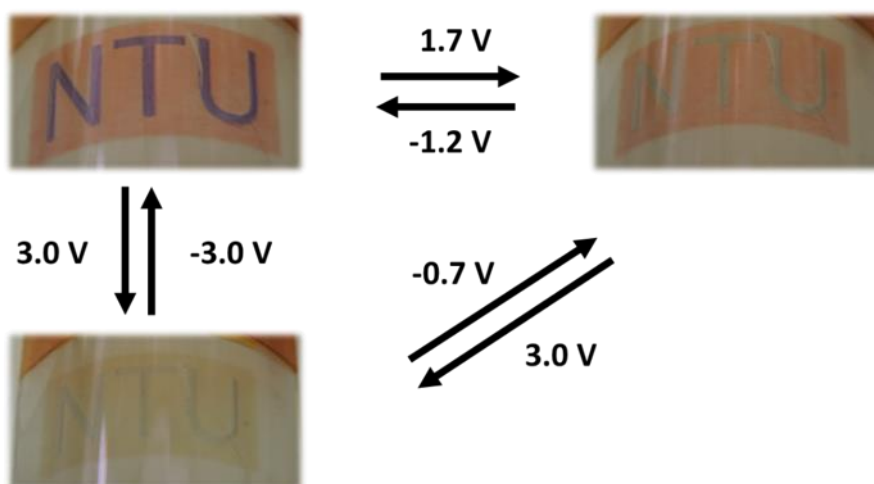
Figure 4.12 Color states of the patterned ECD under bending.

Chapter 5 Conclusion
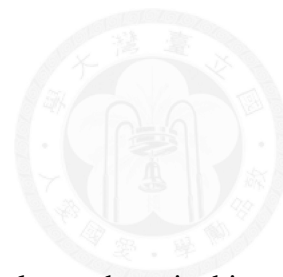
In this thesis, an inkjet printing method is developed to fabricate electrochromic thin films patterns with various colors by adjusting digital printing schemes. MEPE electrochromic materials with different centric metallic ligands are printed on transparent conductive sheets to form electrochromic devices. The FeMEPE EC device shows a great contrast with a transmittance difference (ΔT) of 40.1% at 580 nm, and a high coloration efficiency of 445 cm^2C^{-1} with a short darkening time of 2 s. With a solid electrolyte, the ECDs can be bent and show nearly the same response times and color changes as those without bending. With the advantages of inkjet printing process, printing patterns with multiple colors with excellent precision can be achieved. Herein, by tuning the dot ratios between Ru-MEME and Fe-MEPE inks, one can physically mix the red and blue colorants, and create a series of color gradient transition from red to blue. Besides, the EC materials can also be printed easily at precise locations to create patterns with multiple colors. In summary, this study shows the feasibility of applying inkjet printing technology to fabricate EC thin films with specific colors and patterns, and the fabrication process can be further extended to create flexible multi-color ECD for potential display applications.

Chapter 6 Future Prospect

A seven segment display is produced by the techniques developed in this thesis (Figure 6.1). The water soluble conductive polymer PEDOT (Poly(3,4-ethylenedioxythiophene)) is printed on the flexible substrate PET (Polyethylene terephthalate) as electric circuits and the conductive layer. The EC material FeMEPE was deposited precisely onto the printed PEDOT thin films that it cover the printed conductive layer perfectly. In this device, the metallo-supramolecular polymer can switch between bleached and coloured as those coated on ITO-PEN. The color change of this EC material can still be observed due to the high contrast of MLCT effect even though the similar color that PEDOT and FeMEPE have. This result provides the possibility of further applications in creating flexible electrochromic display.

Figure 6.1 Seven segment display fabricated on PET with PEDOT and FeMEPE.

References

1. Carlson, D.E. and C.R. Wronski, *Amorphous silicon solar cell.* Applied Physics Letters, 1976. **28**(11): p. 671-673.

2. Burroughes, J., et al., *Light-emitting diodes based on conjugated polymers.* nature, 1990. **347**(6293): p. 539-541.

3. Jin, D.U., et al. *65.2: Distinguished Paper: World-Largest (6.5") Flexible Full Color Top Emission AMOLED Display on Plastic Film and Its Bending Properties*. in *SID Symposium Digest of Technical Papers*. 2009. Wiley Online Library.

4. Weisfield, R.L., et al. *New amorphous-silicon image sensor for x-ray diagnostic medical imaging applications*. 1998.

5. Wong, W.S. and A. Salleo, *Flexible electronics: materials and applications*. Vol. 11. 2009: Springer Science & Business Media.

6. Clemens, W., et al., *From polymer transistors toward printed electronics.* Journal of Materials Research, 2004. **19**(07): p. 1963-1973.

7. Perelaer, J., et al., *Printed electronics: the challenges involved in printing devices, interconnects, and contacts based on inorganic materials.* Journal of Materials Chemistry, 2010. **20**(39): p. 8446-8453.

8. Zhou, L., et al., *All-organic active matrix flexible display.* Applied Physics Letters, 2006. **88**(8): p. 3502.

9. Gelinck, G.H., et al., *Flexible active-matrix displays and shift registers based on solution-processed organic transistors.* Nat Mater, 2004. **3**(2): p. 106-110.

10. Comiskey, B., et al., *An electrophoretic ink for all-printed reflective electronic displays.* Nature, 1998. **394**(6690): p. 253-255.

11. Somani, P.R. and S. Radhakrishnan, *Electrochromic materials and devices: present and future.* Materials Chemistry and Physics, 2003. **77**(1): p. 117-133.

12. Mortimer, R.J., *Electrochromic materials.* Chemical Society Reviews, 1997. **26**(3): p. 147-156.

13. Monk, P.M., R.J. Mortimer, and D.R. Rosseinsky, *Electrochromism: fundamentals and applications*. 2008: John Wiley & Sons.

14. Granqvist, C.G., *Handbook of inorganic electrochromic materials*. 1995: Elsevier.

15. Batchelor, R., M. Burdis, and J. Siddle, *Electrochromism in sputtered WO 3 thin films.* Journal of the Electrochemical Society, 1996. **143**(3): p. 1050-1055.

16. Sharpe, A.G., *Chemistry of cyano complexes of the transition metals*. 1976: Academic Press.

17. Neff, V.D., *Electrochemical Oxidation and Reduction of Thin Films of Prussian*

Blue. Journal of The Electrochemical Society, 1978. **125**(6): p. 886-887.

18. Bird, C. and A. Kuhn, *Electrochemistry of the viologens.* Chem. Soc. Rev., 1981. **10**(1): p. 49-82.

19. Schoot, C.J., et al., *New electrochromic memory display.* Applied Physics Letters, 1973. **23**(2): p. 64-65.

20. Garnier, F., et al., *Organic conducting polymers derived from substituted thiophenes as electrochromic material.* Journal of Electroanalytical Chemistry and Interfacial Electrochemistry, 1983. **148**(2): p. 299-303.

21. Pickup, P., *Electrochemistry of Electronically Conducting Polymer Films*, in *Modern Aspects of Electrochemistry*, R. White, J.O.M. Bockris, and B.E. Conway, Editors. 1999, Springer US. p. 549-597.

22. Jang, G.W., et al., *Large‐Area Electrochromic Coatings: Composites of Polyaniline and Polyacrylate‐Silica Hybrid Sol‐Gel Materials.* Journal of The Electrochemical Society, 1996. **143**(8): p. 2591-2596.

23. Beer, P.D., et al., *Cyclic voltammetry of benzo-15-crown-5 ether-vinyl-bipyridyl ligands, their ruthenium (II) complexes and bismethoxyphenyl-vinyl–bipyridyl ruthenium (II) complexes. Electrochemical polymerization studies and supporting electrolyte effects.* Journal of the Chemical Society, Faraday Transactions, 1993. **89**(2): p. 333-338.

24. Mortimer, R.J., A.L. Dyer, and J.R. Reynolds, *Electrochromic organic and polymeric materials for display applications.* Displays, 2006. **27**(1): p. 2-18.

25. Moore, D.J. and T.F. Guarr, *Electrochromic properties of electrodeposited lutetium diphthalocyanine thin films.* Journal of Electroanalytical Chemistry and Interfacial Electrochemistry, 1991. **314**(1–2): p. 313-321.

26. Goldenberg, L.M., *Electrochemical properties of Langmuir—Blodgett films.* Journal of Electroanalytical Chemistry, 1994. **379**(1–2): p. 3-19.

27. Besbes, S., et al., *Electrochromism of octaalkoxymethyl-substituted lutetium diphthalocyanine.* Journal of Electroanalytical Chemistry and Interfacial Electrochemistry, 1987. **237**(1): p. 61-68.

28. Lampert, C.M., *Electrochromic materials and devices for energy efficient windows.* Solar Energy Materials, 1984. **11**(1–2): p. 1-27.

29. Hamnett, A., et al., *A study of the electrodeposition and subsequent potential cycling of Prussian Blue films using ellipsometry.* Journal of Electroanalytical Chemistry and Interfacial Electrochemistry, 1988. **255**(1–2): p. 315-324.

30. Mortimer, R.J. and T.S. Varley, *Electrochromic devices based on surface-confined Prussian blue or Ruthenium purple and aqueous solution-phase di-n-heptyl viologen.* Solar Energy Materials and Solar Cells, 2013. **109**: p. 275-279.

31. Shim, G.H., et al., *Inkjet-printed electrochromic devices utilizing polyaniline–*

silica and poly(3,4-ethylenedioxythiophene)–silica colloidal composite particles. Journal of Materials Chemistry, 2008. **18**(5): p. 594.

32. Costa, C., et al., *Inkjet printing of sol-gel synthesized hydrated tungsten oxide nanoparticles for flexible electrochromic devices.* ACS Appl Mater Interfaces, 2012. **4**(3): p. 1330-40.

33. Beverina, L., G.A. Pagani, and M. Sassi, *Multichromophoric electrochromic polymers: colour tuning of conjugated polymers through the side chain functionalization approach.* Chem Commun (Camb), 2014. **50**(41): p. 5413-30.

34. Alamer, F.A., et al., *Solid-state high-throughput screening for color tuning of electrochromic polymers.* Adv Mater, 2013. **25**(43): p. 6256-60.

35. Han, F.S., M. Higuchi, and D.G. Kurth, *Metallosupramolecular Polyelectrolytes Self-Assembled from Various Pyridine Ring-Substituted Bisterpyridines and Metal Ions: Photophysical, Electrochemical, and Electrochromic Properties.* Journal of the American Chemical Society, 2008. **130**(6): p. 2073-2081.

36. Higuchi, M., *Electrochromic Organic–Metallic Hybrid Polymers: Fundamentals and Device Applications.* Polymer Journal, 2009. **41**(7): p. 511-520.

37. Higuchi, M., *Stimuli-responsive metallo-supramolecular polymer films: design, synthesis and device fabrication.* J. Mater. Chem. C, 2014. **2**(44): p. 9331-9341.

38. Tieke, B., *Coordinative supramolecular assembly of electrochromic thin films.* Current Opinion in Colloid & Interface Science, 2011. **16**(6): p. 499-507.

39. Hu, C.-W., et al., *Multi-colour electrochromic properties of Fe/Ru-based bimetallo-supramolecular polymers.* Journal of Materials Chemistry C, 2013. **1**(21): p. 3408.

40. Bulloch, R.H., et al., *An electrochromic painter's palette: color mixing via solution co-processing.* ACS Appl Mater Interfaces, 2015. **7**(3): p. 1406-12.

41. Granqvist, C.-G., *Electrochromic materials: Out of a niche.* Nat Mater, 2006. **5**(2): p. 89-90.

42. Cho, S.I., et al., *Nanotube-Based Ultrafast Electrochromic Display.* Advanced Materials, 2005. **17**(2): p. 171-175.

43. Kamyshny, A., J. Steinke, and S. Magdassi, *Metal-based inkjet inks for printed electronics.* Open Applied Physics Journal, 2011. **4**: p. 19-36.

44. Singh, M., et al., *Inkjet printing-process and its applications.* Advanced materials, 2010. **22**(6): p. 673.

45. Berggren, M., D. Nilsson, and N.D. Robinson, *Organic materials for printed electronics.* Nature Materials, 2007. **6**(1): p. 3-5.

46. Magdassi, S., M. Grouchko, and A. Kamyshny, *Copper nanoparticles for printed electronics: routes towards achieving oxidation stability.* Materials, 2010. **3**(9): p. 4626-4638.

47. Garnett, E.C., et al., *Self-limited plasmonic welding of silver nanowire junctions.* Nature materials, 2012. **11**(3): p. 241-249.

48. Krebs, F.C., et al., *A complete process for production of flexible large area polymer solar cells entirely using screen printing—first public demonstration.* Solar Energy Materials and Solar Cells, 2009. **93**(4): p. 422-441.

49. Ito, S., et al., *Fabrication of screen-printing pastes from TiO2 powders for dye-sensitised solar cells.* Progress in Photovoltaics, 2007. **15**(7): p. 603.

50. Delaney, J.T., et al., *A Practical Approach to the Development of Inkjet Printable Functional Ionogels—Bendable, Foldable, Transparent, and Conductive Electrode Materials.* Macromolecular rapid communications, 2010. **31**(22): p. 1970-1976.

51. Tekin, E., P.J. Smith, and U.S. Schubert, *Inkjet printing as a deposition and patterning tool for polymers and inorganic particles.* Soft Matter, 2008. **4**(4): p. 703-713.

52. Miller, S.M., S.M. Troian, and S. Wagner, *Direct printing of polymer microstructures on flat and spherical surfaces using a letterpress technique.* Journal of Vacuum Science & Technology B, 2002. **20**(6): p. 2320-2327.

53. Pudas, M., et al., *Gravure printing of conductive particulate polymer inks on flexible substrates.* Progress in Organic Coatings, 2005. **54**(4): p. 310-316.

54. Puetz, J. and M.A. Aegerter, *Direct gravure printing of indium tin oxide nanoparticle patterns on polymer foils.* Thin Solid Films, 2008. **516**(14): p. 4495-4501.

55. Xia, Y. and G.M. Whitesides, *Soft lithography.* Annual review of materials science, 1998. **28**(1): p. 153-184.

56. Unger, M.A., et al., *Monolithic microfabricated valves and pumps by multilayer soft lithography.* Science, 2000. **288**(5463): p. 113-116.

57. Hidber, P.C., et al., *Microcontact printing of palladium colloids: micron-scale patterning by electroless deposition of copper.* Langmuir, 1996. **12**(5): p. 1375-1380.

58. Tate, J., et al., *Anodization and microcontact printing on electroless silver: Solution-based fabrication procedures for low-voltage electronic systems with organic active components.* Langmuir, 2000. **16**(14): p. 6054-6060.

59. Dong, H., W.W. Carr, and J.F. Morris, *An experimental study of drop-on-demand drop formation.* Physics of Fluids (1994-present), 2006. **18**(7): p. 072102.

60. Grove, M., et al., *Color flat panel manufacturing using ink jet technology.* Display Works, 1999. **99**.

61. Shah, V.G. and D.J. Hayes, *Trimming and printing of embedded resistors using demand-mode ink-jet technology and conductive polymer.* IPC Printed Circuit

Expo, 2002: p. 1-5.

62. Wallace, D., et al. *Ink-jet as a MEMS manufacturing tool*. in *2007 First International Conference on Integration and Commercialization of Micro and Nanosystems*. 2007. American Society of Mechanical Engineers.

63. Hayes, D.J., D.B. Wallace, and W. Royall Cox. *MicroJet printing of solder and polymers for multi-chip modules and chip-scale packages*. in *Proceedings-SPIE the International Society for Optical Engineering*. 1999. Citeseer.

64. Le, H.P., *Progress and trends in ink-jet printing technology*. Journal of Imaging Science and Technology, 1998. **42**(1): p. 49-62.

65. Brünahl, J. and A.M. Grishin, *Piezoelectric shear mode drop-on-demand inkjet actuator*. Sensors and Actuators A: Physical, 2002. **101**(3): p. 371-382.

66. Lee, K.H., et al., *"Cut and stick" rubbery ion gels as high capacitance gate dielectrics*. Adv Mater, 2012. **24**(32): p. 4457-62.